https://doi.org/10.5194/essd-2026-697
Preprint. Discussion started: 18 September 2026

Open Access Earth System Science Data Discussions

MioMG: Reconstructing robust ocean temperatures from Miocene foraminiferal Mg/Ca records

Sindia M. Sosdian[1], Karlos G. D. Kochann[2,3], Anya V. Hess[4], Clara Bolton[5], Anna Joy Drury[6,7], Emily J. Judd[8], Wolfgang Kuhnt[9], Caroline H. Lear[1], Paul Minton[7], Alexandra Auderset[10], Sevasti Modestou[11], Ann Holbourn[9, †]

[1] School of Earth & Environmental Sciences, Cardiff University, Cardiff, UK
[2] GEOMAR Helmholtz Centre for Ocean Research Kiel, Kiel, Germany
[3] Technological Institute on Paleoceanography and Climate Change (itt OCEANEON), UNISINOS University, São Leopoldo, Brazil
[4] College of Science, George Mason University, Fairfax, Virginia, USA
[5] Aix Marseille Univ, CNRS, IRD, INRAE, CEREGE, Aix-en-Provence, France
[6] School of Geography, Geology and the Environment, University of Leicester, Leicester, UK
[7] Department of Earth Sciences, University College London, London, UK
[8] Earth Sciences New Zealand, Auckland, NZ
[9] Institute for Geosciences, Kiel University, Kiel, Germany
[10] School of Ocean and Earth Sciences, University University of Southampton, Southampton, UK
[11] Department of Geography and Earth Sciences, Northumbria University, Newcastle, UK
† Deceased

Correspondence: Sindia Sosdian (SosdianS@cardiff.ac.uk)

Abstract. Paleoclimate records from the Miocene epoch (~5.3 to ~23.0 Million years ago) present an opportunity to assess the Earth's climate system under a warmer-than-modern mean state, when atmospheric CO_2 levels were within the range of those projected for the next century under intermediate climate change scenarios. Ocean temperature is a key climate system parameter because latitudinal temperature gradients provide critical information on the climate system and potential carbon cycle feedbacks in the geological past. Over the last several decades, magnesium-to-calcium (Mg/Ca) ratios in both planktic and benthic foraminiferal shells have been applied as a temperature proxy providing insight into spatial and temporal change in upper ocean and bottom water temperature across the Miocene. However, Miocene climate models struggle to reconstruct the reduced latitudinal temperature gradient inferred from available proxy records, including those based on Mg/Ca. Further, recent advances in planktic and benthic foraminiferal Mg/Ca-temperature paleothermometry show that non-thermal factors and seawater chemistry need to be considered when converting Mg/Ca to temperature. Here, we present the MioMG temperature compilation, led by the Mg/Ca working group within the international MioOcean community effort. Fifty-two Miocene foraminiferal Mg/Ca records from both planktic and benthic foraminifera were reevaluated and temperatures were recalculated to provide robust, consistent temperature estimates including uncertainties. Conversion of planktic and benthic Mg/Ca to temperature requires consideration of carbonate chemistry sensitivity for individual species, sensitivity of foraminiferal Mg/Ca to the Mg/Ca seawater composition (Mg/Ca_{sw}), and appropriate calibration. We compiled records of the seawater Mg/Ca composition (Mg/Ca_{sw}), based on a diverse set of proxies, and present this record for use in future application of Mg/Ca-derived Miocene temperature reconstructions. Miocene Mg/Ca records are derived from extant and extinct foraminiferal species. Further, preservation information is essential to determine the quality of reconstructions. Our recalculated upper ocean temperature (UOT) estimates showcase warm Middle Miocene temperatures and a cooling trend towards the Late Miocene. Revised bottom water temperature (BWT) estimates also depict warm Middle Miocene values followed by a cooling trend, which is consistent among sites located at different paleodepths. Overall, absolute temperature estimates are higher than previously published estimates due to application of corrections based on the updated MioOcean Mg/Ca_{sw} curve. The MioMG compilation is presented on an interactive Streamlit-based web platform allowing for exploration of the data for

https://doi.org/10.5194/essd-2026-697
Preprint. Discussion started: 18 September 2026

Open Access Earth System Science Data Discussions

specialists and non-specialists to aid in application of dataset for Miocene researchers. The dataset is publicly available at Zenodo (https://doi.org/10.5281/zenodo.22258386, Sosdian et al. 2026).

1 Introduction

The dynamic climate of the Miocene provides a unique opportunity to understand climate processes and feedbacks in a warmer-than-modern mean climate state with persistent polar glaciation. Indeed, the Miocene Climatic Optimum (MCO; 16.9-14.7 Ma) represents an analog for intermediate future climate change scenario (RCP 4.5 or 6.0) (Steinthorsdottir et al. 2021). Despite its high potential to serve as an analogue for future climate, discrepancies between temperature proxy data and climate model simulations, and between different proxy systems, limit our understanding of Earth's climate dynamics during the Miocene. For example, Miocene climate models are unable to reproduce the reduced latitudinal temperature gradient derived from ocean temperature records (Burls et al. 2021), and discrepancies between temperature estimates derived from different proxy systems can further complicate the interpretation of Miocene climate records. In addition, individual studies based on the same paleotemperature proxy may use different equations and correction frameworks. These inconsistencies highlight the need to incorporate recent advances into proxy systematics to produce higher confidence ocean temperature estimates, providing clearer insights into the Miocene climate, and helping to constrain climate models and processes. MioOcean (see Sosdian et al., this volume) is an international coordinated ocean-temperature compilation effort, which aims to review proxy systematics and refine temperature estimates for five proxy archives, namely TEX_{86}, $U^{K'}_{37}$, foraminiferal $\delta^{18}O$, foraminiferal Δ_{47}, and foraminiferal Mg/Ca, while facilitating intercomparison through the use of a revised and consistent age framework. Here, we propose a consistent workflow for robustly applying the Mg/Ca-paleothermometer measured on foraminiferal tests to reconstruct upper and deep ocean temperatures across the Miocene.

The Mg/Ca paleothermometer is based on thermodynamic experiments that showed that the degree of Mg^{2+} substitution for Ca^{2+} in the crystal lattice of calcium carbonate (calcite) increases with fluid temperature (Clarke et al.,1922; Chave et al.,1954; Chilingar et al.,1962). Further work demonstrated that this relationship also holds in biogenic carbonates, such as the tests precipitated by foraminifera (unicellular oceanic protists), though the Mg/Ca-temperature (Mg/Ca-T) sensitivities differ between species. Calibrations relating changes in foraminiferal Mg/Ca values with changes in water temperature are based on measurements from modern benthic and planktic foraminifera that live at different water depths and latitudes in the ocean and obtained from core-tops, sediment traps, and plankton nets, as well as those grown in culture (e.g., Nürnberg et al., 1996; Lear et al., 2002; Anand et al., 2003). These species-specific relationships, which are usually expressed as exponential functions, have been used to reconstruct temperature variations on a range of timescales (seasonal to million years (Myr)), time intervals (Holocene to Late Cretaceous), and water column depths (e.g., Lear et al., 2010; Cramer et al., 2009). When coupled with oxygen isotope ($\delta^{18}O$) data, the Mg/Ca paleothermometer can be used to estimate changes in the $\delta^{18}O$ of seawater in the upper and deep ocean, which are driven by salinity, local hydroclimate, water mass mixing, and ice volume variations in the open ocean (e.g., Elderfield & Ganssen, 2000; Lear et al., 2000).

The Mg/Ca proxy was first applied to Miocene records in the early 2000s; however, several challenges have arisen when extending the proxy deeper in geologic time, particularly for timescales that exceed the residence time of Mg in the ocean (~13 Myrs). Importantly, both planktic and benthic foraminiferal Mg/Ca are sensitive to changes in the Mg/Ca composition of seawater (Mg/Ca_{sw}) as well as species-specific sensitivity to environmental conditions (e.g., pH, salinity, carbonate ion saturation). On millions-of-years timescales, both proxy and modelling reconstructions indicate a long-term increase in Mg/Ca_{sw} from the early Cenozoic to a present day value of 5.2 mol/mol (Hardie, 1996; Higgins & Schrag 2012; Higgins & Schrag 2015; Fantle & DePaolo 2006; Horita et al. 2002; Dickson, 2002, 2004; Brennan et al. 2013; Coggon et al. 2010; Rausch et al. 2013; Gothmann et al. 2015; Evans et al. 2018; Evans et al. 2026). Previous work has shown that the relationship between Mg/Ca_{sw} and Mg/Ca in foraminiferal calcite is described by a power function as outlined in eq. 1,

https://doi.org/10.5194/essd-2026-697
Preprint. Discussion started: 18 September 2026

where F is a function that includes the sensitivity to temperature and H is a constant, each determined for each species:

$$Mg/Ca_{calcite}=F \times Mg/Ca_{sw}^{H} \qquad \text{Eq. (1)}$$

The *H*-value has been shown to be species-specific, with a variety of approaches resulting in *H*-value estimates ranging from 0.41 (Delaney et al. 1985) to 1.00 (Tierney et al. 2019) in planktic foraminifera and from 0.27 to 1.00 in benthic foraminifera (Lear et al. 2000; Billups & Schrag, 2003; Segev and Erez, 2006; Lear et al., 2015). In addition to changing Mg/Ca_{sw}, non-thermal factors can influence Mg/Ca (Lea et al., 1999; Elderfield et al. 2006; Kisakürek et al. 2008; Dueñas-Bohórquez et al., 2009; Hönisch et al., 2013). Reconstructing Miocene ocean temperatures derived from extinct foraminiferal taxa leads to additional challenges such as lack of modern species analog and limited constraints on species-specific offsets and vital effects. For planktic Mg/Ca recent work has shown that multi-variable calibrations are needed to account for sensitivity to pH for some species (e.g., *Globigerina bulloides*) and salinity (Gray & Evans, 2019; Tierney et al. 2019; Holland et al. 2020). Applying these calibrations to reconstruct paleotemperatures is challenging due to the absence of site-specific records of past pH and salinity. For instance, there are no direct proxies for salinity, especially during the Miocene, while boron isotope-derived proxies indicate changes in ocean pH across this time interval (Sosdian et al., 2018; Whiteford et al. 2024).

For benthic Mg/Ca, bottom water temperature (BWT) reconstructions based on Mg/Ca are sensitive to changes in deep ocean carbonate chemistry. Carbonate saturation state is the main factor that can bias temperature estimates, impacting the Mg partitioning in the benthic foraminiferal $CaCO_3$ shell, systematically lowering Mg/Ca ratios with decreasing carbonate saturation (e.g., Martin et al., 2002; Rosenthal et al., 2006; Elderfield et al., 2006; Healey et al., 2008; Raitzsch et al., 2008; Yu and Elderfield, 2008; Regenberg et al., 2014). However, recent work has demonstrated that infaunal benthic foraminifera exhibit lowered sensitivity to carbonate saturation state changes than epifaunal species due to a buffering effect of pore waters (Elderfield et al. 2010; Lear et al. 2015), implying that they can be used to reconstruct high confidence BWTs.

Reconstructing temperatures from Mg/Ca records also requires a thorough assessment of diagenesis. The main processes impacting preservation of the primary biogenic signal include dissolution, overgrowth with inorganic calcite or oxide coatings, recrystallisation, and infilling. These processes are driven by site-specific conditions, including sedimentology, burial depth, sedimentation rates, and pore fluid geochemistry that impact the interaction between the biogenic calcite and the surrounding pore fluids (Sexton et al., 2006, Sexton and Wilson, 2009; Edgar et al., 2013, Edgar et al., 2015). Foraminifera in clay-rich sediments generally preserve better than those in sediments with a higher carbonate content, as a higher clay content will reduce permeability and minimise the impact of contact with post depositional fluids with a different composition (Pearson et al., 2001, Wilson and Norris, 2001). The degree to which pore waters are buffered with respect to carbonate saturation state can also impact benthic foraminiferal Mg/Ca (Lear et al., 2015). Greater burial depth will expose material to greater geothermal warmth, making it more likely that the original temperature signature may be overprinted by that of any new calcite precipitation or recrystallization. The location of an individual study site and the local pore fluids' chemistry also impact the effects of post-depositional processes on the preservation of the primary foraminiferal Mg/Ca signal. Monitoring post-depositional impacts on primary Mg/Ca can be complicated by the fact that, for instance in some areas of the Pacific Ocean, pore water Mn concentrations are higher compared to other ocean basins. This could lead to Mn/Ca values that would ordinarily be above the cut-off threshold for consideration, even though the Mg/Ca values remain unaffected (Sosdian et al., 2020).

Considering all of the factors outlined above, revisiting best approaches to reconstructing Miocene upper and deep ocean temperatures is necessary. Here, we present a new Miocene foraminiferal Mg/Ca compilation that includes 52 globally distributed published records spanning some or all of the Miocene (Figures 1, 2). As part of the MioOcean effort, we provide a refined framework to convert foraminiferal Mg/Ca to ocean temperature in these records, including calibration, Mg/Ca_{sw}

https://doi.org/10.5194/essd-2026-697
Preprint. Discussion started: 18 September 2026

correction, and accounting for changes in carbonate chemistry, salinity, and preservation. Our Mg/Ca-temperature data compilation product includes methodological recommendations for using Miocene foraminiferal Mg/Ca to produce robust Miocene ocean temperature estimates. The compiled data and reconstructed temperatures are available through a Streamlit web application, enabling users to explore and visualize the data product across Mg/Ca-temperature calibrations and key input parameters.

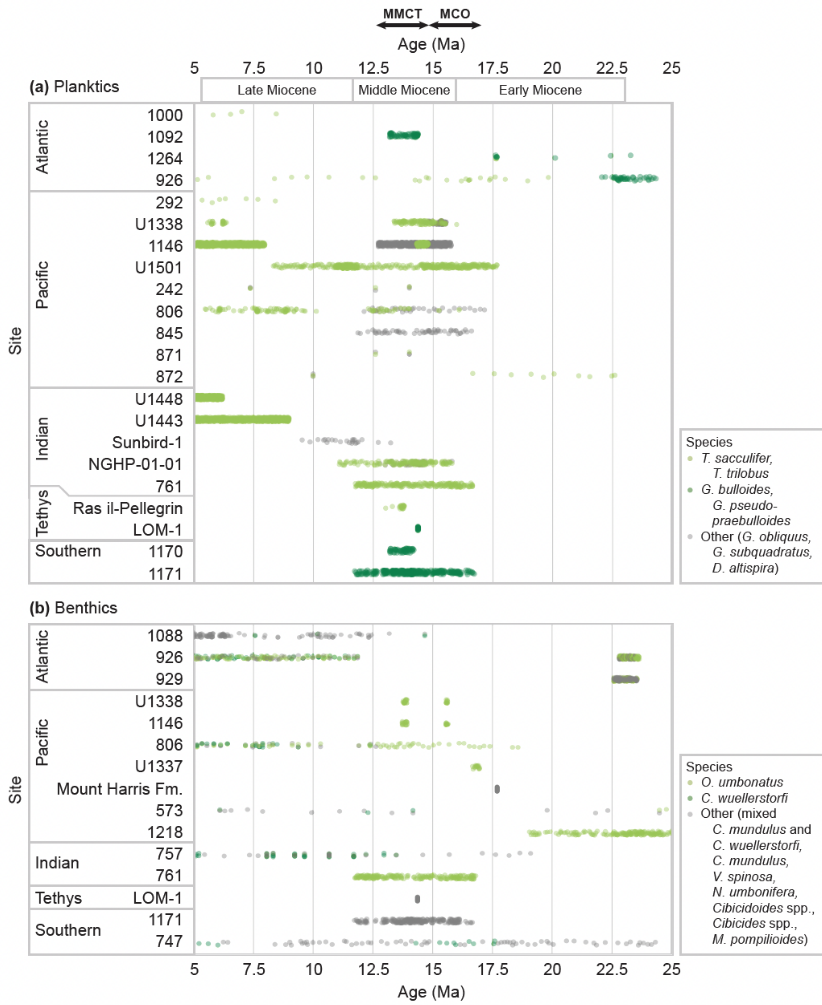

Figure 1. Spatial distribution and temporal duration and resolution of (a) planktic and (b) benthic Mg/Ca records. Coloured by confidence and species in the Mg/Ca-derived temperature estimates, where light green is the most confident, dark green is moderately confident, and gray is uncertain.

https://doi.org/10.5194/essd-2026-697
Preprint. Discussion started: 18 September 2026

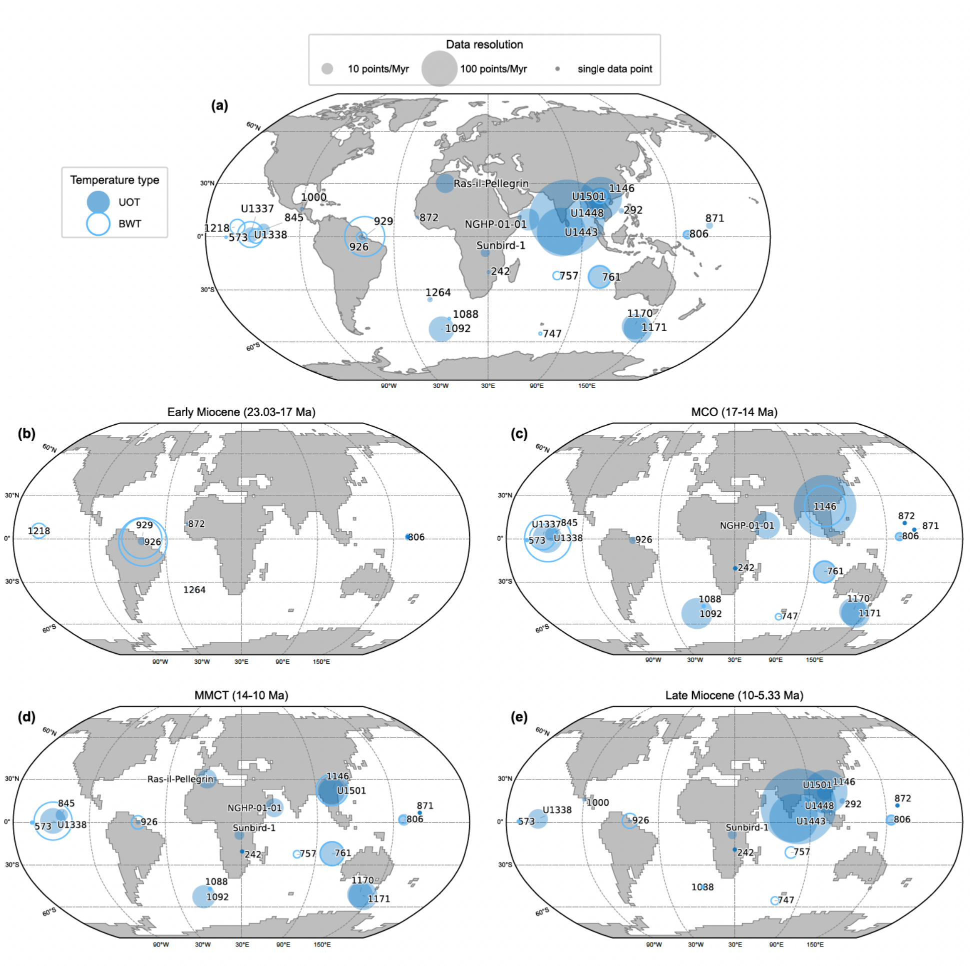

Figure 2. Paleolocations of Mg/Ca proxy sites from the MioOcean compilation across the Miocene. (a) All sites spanning 23.03–5.33 Ma shown on the modern geography; (b–e) sites shown on MioMIP2 phase 2 paleogeography for four intervals: (b) Early Miocene (23.03–17 Ma), (c) Miocene Climatic Optimum (17–14 Ma), (d) Middle Miocene Climate Transition (14–10 Ma), and (e) Late Miocene (10–5.33 Ma). Blue filled circles denote upper ocean temperature (UOT) records and blue open rings denote bottom water temperature (BWT) records. Marker size is proportional to data resolution (number of data points per million years); small, filled dots mark single-data-point sites for which resolution cannot be computed. Paleocoordinates are the mean of the oldest and youngest reconstructed positions within each interval.

2 Methods

2.1 Data sources

Planktic and benthic foraminiferal Mg/Ca data were compiled from published studies (Year 2000 to present) (Supplementary Table S1-S2) available in online data repositories or as supplementary data files from Deep Sea Drilling Project (DSDP), Ocean Drilling Program (ODP), Integrated Ocean Drilling Program (Integrated ODP; 2003-2013), International Ocean Discovery Program (International ODP; 2013-2024), and onshore drilling sites. Initially, we reviewed records on the Bolin Temperature Portal, an online platform that houses available Miocene ocean temperatures,

https://doi.org/10.5194/essd-2026-697
Preprint. Discussion started: 18 September 2026

as a starting point to compile a list of all records (Lawrence et al. 2020; Sosdian et al. 2024). We compiled proxy values, published temperature estimates, and proxy-specific metadata, including taxon name, size fraction, instrument type, trace metal cleaning method, and contamination information where available, typically used to assess whether Mg/Ca values retain a primary and/or been influenced by diagenetic processes. Note that some datasets did not report temperature estimates and/or associated uncertainties in the original publication. To assess site-specific environmental and climate conditions, we reviewed modern temperature, salinity, and carbonate chemistry parameters, including calcite saturation, derived from the gridded Global Ocean Data Analysis Project (GLODAP) data product (Version 2; Lauvset et al., 2016). These data were used to compare modern temperatures with calculated values, characterize modern salinity, and assess the saturation state of sites used for both planktic and benthic data. Parameters for sites located on land were extracted from oceanographic data from the nearest ocean grid cell.

For this contribution, preservation summaries were extracted from previous work where available (38 out of 52 sites) and used as a guide at each site for consideration of the temperature output (see Supplementary Tables S1-S2). Preservation information was collated at a site level, but each publication was kept separate, as studies frequently cover different time periods and preservation state can vary downcore. The preservation state and/or assessment reported by the authors was summarised based on the main manuscript and supplementary information including method or approach used. Additionally, a literature review was completed for each site to identify any available SEM images, as well as any other studies reporting on foraminiferal preservation of the site. For SEM images, we collated information about image availability following the recommended approach outlined in literature (Appendix A: Fig. A1; Sexton et al., 2006; Rosenthal et al., 2018) such as whether images were available for the whole test, wall structure and/or for multiple time intervals. This approach provides a systematic way of identifying dissolution, calcite overgrowths, recrystallisation and infilling, and can be used to identify downcore variations in preservation. However, it remains difficult to identify secondary coatings and to quantify the actual impact of the preservation state on the test geochemistry.

2.2 Data Coverage

Published Miocene planktic foraminiferal Mg/Ca temperature data are available from 18 DSDP/ODP/Integrated ODP/International ODP drilling sites, an additional Indian NGHP deep-ocean site, and two onshore locations in the Tethys/Paratethys (Supplementary Table S1-S2. Figure 1, 2). Six sites are located in the Pacific Ocean (DSDP Site 292, ODP Sites 806, 845, 871, 872, and Integrated ODP Site U1338; Sato et al. 2008, Nathan and Leckie, 2009, Sosdian and Lear, 2020, Hess et al. 2023, Boscolo-Galazzo et al. 2021, Sosdian et al. 2018, Greenop et al. 2019, Fox 2014 [Data provided by author], Fox et al. 2021, Drury et al. 2018, Guillermic et al. 2022; Liu et al. 2022), two sites in the South China Sea (ODP Site 1146 and International ODP site U1501; Steinke et al. 2010, Holbourn et al. 2010, 2018; Yang et al. 2021, Yang et al. 2026), four sites in the Atlantic Ocean (ODP Sites 926, 1000, 1092 and 1264; Foster et al. 2012, Sosdian et al. 2018, Greenop et al. 2019, Kuhnert et al. 2009, Anderson et al. 2024), five sites in the Indian Ocean (DSDP Site 242, ODP sites 761, Integrated ODP Sites U1443 and U1448, NGHP-01-01; Boscolo-Galazzo et al. 2021, Sosdian et al. 2018, Sosdian et al. 2020, Foster et al. 2012, Martinot et al. 2022, Jöhnck et al. 2020, Yang et al. 2020, Zou et al. 2022), three sites in the Southern Ocean (ODP Sites 747, 1170 and 1171; Verducci et al. 2007, Shevenell et al. 2004), and three onshore sites (LOM-1 in Czechia, Ras il-Pellegrin (RIP) in Malta and Sunbird-1 in Tanzania; Scheiner et al. 2018, Badger et al. 2013, Nairn et al. 2021). Modern water depths range between ~720 m and 4200 m. Note for ODP Site 747 dataset (Verducci et al. 2007; Verducci et al 2009), Mg/Ca data are not available from a repository, so we compiled only the available metadata for comparison with other records.

The age resolution varies from 3.0 kiloyear (kyr) to nearly 1.0 Myr, and the Early Miocene is less well represented (201 data points) in the data than the Middle (2035 data points) and Late Miocene (2015 data points). To reconstruct Mg/Ca_{sw} we compiled planktic foraminiferal Na/Ca records from published work (Zhou et al. 2021; Rosenthal et al. 2022). The Miocene Na/Ca record is derived

https://doi.org/10.5194/essd-2026-697
Preprint. Discussion started: 18 September 2026

from ten sites including: DSDP 608 and 667; ODP 758, 806, 807, 925, 926, 1237, 1264; Integrated ODP U1337.

Published Miocene benthic Mg/Ca temperature data are available from 13 DSDP/ODP/Integrated ODP drilling sites and two onshore locations (Table A1-A2). Six sites are located in the Pacific Ocean (DSDP Site 573, ODP Sites 806, 1218, Integrated ODP Sites U1337 and U1338; Lear et al. 2000, 2003, 2004, 2015, Kochhann et al. 2017), including one on-shore location in New Zealand (Mount Harris; Fukuda et al., 2012), and three sites are located in Atlantic Ocean (ODP Sites 926, 929, 1088; Lear et al. 2003, Mawbey & Lear 2013, Billups & Scheiderich 2009), two in the Indian Ocean (ODP Sites 757 and 761, Billups & Schrag 2003, Lear et al. 2010) and Southern Ocean (ODP Sites 747 and 1171; Billups & Schrag 2002, Shevenell et al. 2008), and one (ODP Site 1146; Kochhann et al. 2017) in the South China Sea, a Pacific marginal sea that was part of the subtropical NW Pacific during most of the Miocene. The other onshore location, LOM-1, is located in Paratethys. The majority of these locations record deep-water temperatures in bathyal to abyssal water depths, with the exception of ODP Sites 747 and 757 in the Southern and Indian Ocean, respectively, that were bathed in upper deep to intermediate water in the Miocene. The Mount Harris Site is the only location bathed by shallow water (outer shelf, 100-200 m paleo-water depth). The age resolution varies from ~4.9 kyr to ~883.0 kyr, and the Late Miocene is less well represented (309 data points) in the data than the Early (413 data points) and Middle Miocene (510 data points).

We assessed the spatial and temporal distribution of the compiled Mg/Ca records to characterize the geographic and temporal coverage of available upper and deep ocean temperature estimates. Records were considered in the context of their oceanographic setting, water depth, latitude, and temporal resolution, allowing us to identify regions and intervals that are relatively well represented as well as those for which fewer records are available.

2.3 Age model framework

A consistent MioOcean Age Framework was developed by a separate working group of the MioOcean effort (MioAGE: Drury et al., this volume). Briefly, following a critical age model survey classifying all MioOcean sites and UOT/BWT records (including Mg/Ca), the age models for 38 key sites were revised, verified and standardised within the MioOcean Age Framework anchored to the GTS2012 timescale (Hilgen et al., 2012) or astrochronology. All Mg/Ca records published at key sites fall within the MioOcean Age Framework, with the age models available in the age model database (key sites with Mg/Ca data: ODP Sites 747, 761, 806, 872, 925, 926, 1088, 1092, 1146, 1170, 1171, 1264 and Integrated ODP Sites U1337, U1338, U1443 and International ODP Site U1501; Drury et al., this volume). For non-key sites, we use the Mg/Ca data on their original published age models. Thus, throughout this contribution, all figures and data analyses use the "MioOcean recommended age (Ma)", which corresponds to the revised MioOcean Age Framework for key sites and the original published age model for non-key sites. The "Published age (Ma)" and "MioOcean recommended age (Ma)" are provided in the accompanying database (see Drury et al., this volume). Note for the land section LOM-1, we compiled Mg/Ca data from both planktic and benthic species, however we did not calculate temperature due to a lack of age model constraints (Scheiner et al. 2018). Sites characterized by modern carbonate undersaturation or intervals affected by carbonate dissolution may warrant particular caution when interpreting BWT estimates such as MCO thermal maximum interval from Integrated IODP site U1338 (Kochhann et al., 2017).

2.4 Data description and availability

The MioMG compilation is released as part of the MioOcean database; a full description of the database structure, file formats, column definitions, units, and quality flags is provided in the companion MioOcean database paper (Sosdian et al., this volume). In brief, the Mg/Ca records are distributed as a proxy-specific file (mgca_product.xlsx) containing the raw Mg/Ca measurements along with the full suite of calibration outputs and associated metadata. Each file is organised into three worksheets: a Data sheet with all sample-level measurements and calculated temperatures; a Columns sheet defining every column name, data type, and unit; and a Metadata sheet documenting

https://doi.org/10.5194/essd-2026-697
Preprint. Discussion started: 18 September 2026

Open Access Earth System Science Data Discussions

provenance (compilation date, input-file hash, and Git commit). Both the published and MioOcean-recommended ages are reported ("Published age (Ma)" and "MioOcean recommended age (Ma)"). The same records are also integrated into the reduced multi-proxy compilation (mio_ocean_product.xlsx), which retains a single recommended (or Monte Carlo–ensemble) calibration per proxy for cross-proxy and model–data comparison (See Section 3.4). The dataset is version-controlled on GitHub (https://github.com/audersea/mio_compilation), archived on Zenodo (https://doi.org/10.5281/zenodo.22258386, Sosdian et al. 2026) and can be downloaded from the MioOcean website (https://www.miocean.com/download-data/). Further the MioMG compilation can be explored interactively via the MioMG (https://mio-mg.streamlit.app/).

2.5 Foraminiferal taxonomy & ecology

2.5.1 Planktic foraminifera

Miocene planktic Mg/Ca records encompass a range of modern, extant morphotypes, and extinct species (Table A1; Figure 1). When assigning calibration relationships, we considered taxonomic and phylogenetic relationships among planktic foraminiferal species, following published frameworks (e.g., Aze et al., 2011; Wade et al. 2011; Spezzaferri et al., 2018a, b; Boscolo-Galazzo et al. 2025; Lamyman et al., 2026). Planktic foraminifera used to reconstruct UOT include the modern species (*Trilobatus sacculifer*, *Globigerina bulloides)*, extant morphotypes (*Trilobatus quadrilobatus, Trilobatus trilobus*), and other extinct species (*Globoturborotalita pseudopraebulloides, Dentoglobigerina altispira, Globigerinoides obliquus, Globigerinoides subquadratus)*.

Trilobatus sacculifer is a spinose surface-dwelling species, with a mixed-layer depth habitat (0-50 m depending on region; Chaabane et al. 2026) that bears photosynthetic symbiotic algae and appeared in the Early Miocene (Kennett and Srinivasan, 1983). The *Trilobatus sacculifer*-group, reassigned from *Globeriginoides* after Spezzaferri et al. (2015), initiated in the early Miocene (22.5 Myrs), including extant morphotypes *T. trilobus* and *T. quadrilobatus*. *T. trilobus* is abundant throughout the Middle and Late Miocene and has been used routinely to reconstruct UOT (Sosdian et al. 2020; Martinot et al. 2022; Holbourn et al. 2018; Johnck et al. 2020). *G. bulloides*, a non-symbiont bearing foraminifera that appeared in the Late Oligocene (Spezzaferri et al. 2018a), generally inhabits the upper 50 m of the water column but has been shown to dwell at deeper depths (~0-75m; Chaabane et al. 2026). We apply the modern *T. sacculifer* Mg/Ca–temperature calibration to *T. trilobus* and *T. quadrilobatus*, and the modern *G. bulloides* calibration to Miocene records (See Section 2.6.2)

The extinct species *Dentoglobigerina altispira* is thought to have been a near-surface dweller (lower mixed-layer and/or upper thermocline) that probably hosted symbionts and is present in the fossil record from the Late Oligocene to the Late Pliocene (Pearson & Shackleton, 1995; Sosdian & Lear, 2020; Zou et al. 2022). *Globoturborotalita pseudopraebulloides* is an extinct species ranging from the early Oligocene to middle Miocene (Spezzaferri et al., 2015, 2018b). It has been inferred to host photosynthetic symbionts (Pearson & Wade, 2009; Andersen et al., 2024) and to exhibit relatively low sensitivity to pH (Andersen et al., 2024). Although previously referred to as *Globigerina sp.* cf. *G. bulloides* by Pearson and Wade (2009), *G. pseudopraebulloides* is now recognised as a distinct species rather than a morphospecies of *G. bulloides* (Spezzaferri et al., 2018b). Lesser-known extinct species used for Mg/Ca records and thought to be a surface dweller are *Globigerinoides obliquus* (Early Miocene-Pleistocene) and *G. subquadratus* (Early–Late Miocene; Spezzaferri et al., 2018b; Shevenell et al. 2004; Holbourn et al. 2021). *G. subquadratus* (Early–Late Miocene) is closely related to *G. ruber* and considered part of an ancestor–descendant pair, with recent Mg/Ca evidence supporting a consistent temperature response between them (Boscolo-Galazzo et al., 2025). For extinct species without a modern equivalent, we apply multispecies or pooled calibrations where appropriate, as outlined below; for *G. subquadratus*, however, we also consider *G. ruber* as a close modern analogue (See Section 2.6.2). ODP Site 1264 Mg/Ca data derive from both Miocene and Oligocene data. For completeness, we compiled all Mg/Ca data including extinct species *Ciperoella angulisuturalis* covering the Oligocene time interval.

https://doi.org/10.5194/essd-2026-697
Preprint. Discussion started: 18 September 2026

We did not apply any size fraction corrections to the data when converting planktic Mg/Ca to temperature. Most Mg/Ca records utilized size fractions within the 250-355 µm range, with the exception of three studies that used a smaller or larger range (ODP Site 1092, 1146, and in; Kuhnert et al. 2009; Steinke et al. 2010; Drury et al. 2018). At ODP Site 1146 (Steinke et al., 2010), the Mg/Ca dataset is based on combined species (*T. sacculifer and T. quadrilobatus)* and there is no size fraction study that has examined *T. quadrilobatus*. For ODP Site 1092 (Kuhnert et al. 2009), we apply no size fraction correction as previous studies show an offset with size fraction, but the magnitude of Mg/Ca difference is variable (Elderfield et al. 2002; Friedrich et al. 2012). For Integrated ODP Site U1338 (Drury et al. 2018), *T. sacculifer* data derives from a range of size fractions. Previous work has found that *T. sacculifer* Mg/Ca increases with size fraction (Recent: Elderfield et al. 2002; Late Miocene: Drury et al. 2018), and size correction factors were calculated for this species (1.13: 355-425 µm and 1.25: 425-500 µm; Drury et al. 2018). On the other hand, *T. trilobus* was shown to have no consistent Mg/Ca trend with test size in Late Miocene samples (Martinot et al 2022). We recommend using 250-300µm Mg/Ca data from Drury et al. (2018) as it falls within the overall range of other studies and covers the Late Miocene time interval.

2.5.2 Benthic foraminifera

Miocene benthic foraminiferal Mg/Ca records have been published for the species *Oridorsalis umbonatus*, *Cibicidoides wuellerstorfi*, *Cibicidoides mundulus*, *Cibicides* spp., *Cibicidoides* spp., *Nuttallides umbonifera*, *Notorotalia spinosa,* and *Melonis pompilioides* (Table A2). For this effort, we only calculated new BWTs for *O. umbonatus*, *C. wuellerstorfi,* and mixed-species derived from combined *C. wuellerstorfi* and *C. mundulus* Mg/Ca measurements.

Oridorsalis umbonatus is a shallow infaunal cosmopolitan species, inhabiting lower neritic to abyssal water depths (Tjalsma and Lohman, 1983; Thomas, 1990; Jones, 1994; Holbourn et al., 2013). It is an extant species that first appeared during the Paleocene (Tjalsma and Lohman, 1983) and became relatively common in deep sea sediments after the middle Eocene (Thomas, 1990). Due to its infaunal microhabitat, *O. umbonatus* Mg/Ca values are less affected by carbonate saturation state, but only at sites where carbonate-rich sediments provide a buffering effect to pore waters (e.g., Lear et al., 2015; Nauter-Alves et al. 2025).

Cibicidoides wuellerstorfi, recently assigned to *Lobatula wuellerstorfi* (Burkett et al., 2025; Nauter-Alves, 2025) and formerly also known as *Planulina wuellerstorfi (*Holbourn et al., 2013), is an extant epifaunal species that inhabits bathyal water depths (Holbourn et al., 2013). It has a cosmopolitan distribution, and first appeared at ~16.0 Ma, in the Middle Miocene (Holbourn et al., 2013). Some studies, such as the record from ODP Site 747 (Billups and Schrag, 2002) report *C. wuellerstorfi* data from before their accepted first appearance, suggesting that the species attribution may be incorrect. We therefore opted to only recalibrate *C. wuellerstorfi* Mg/Ca data younger than 16.0 Ma, though data points older than 16.0 Ma remain in the database and their originally published paleotemperatures are available. For sites with mixed-species Mg/Ca measurements on *C. wuellerstorfi* and *C. mundulus*, we have provided BWTs calculated with our revised *C. wuellerstorfi* calibration in the proxy-specific compilation, but we do not consider them to be high confidence temperature estimates.

We did not include *C. mundulus* Mg/Ca records in the MioOcean compilation, since this species's sensitivity to temperature is low (Yu and Elderfield, 2008; Nauter-Alves et al. 2025), with a likely higher sensitivity to carbonate ion concentration changes. Similarly, there are no BWTs calculated for *Cibicides* spp. since the temperature sensitivity of the mixed sample cannot be determined. *N. umbonifera*, *N. spinosa* and *M. pompilioides* Mg/Ca records were not converted to BWT within the MioOcean initiative due to the paucity of calibration studies. Nevertheless, *Cibicidoides mundulus*, *Cibicides* spp., *Cibicidoides* spp., *N. umbonifera*, *N. spinosa* and *M. pompilioides* Mg/Ca records are reported in the MioOcean database as the originally published proxy values and BWT estimates for documentation.

Benthic foraminiferal Mg/Ca records were usually measured on specimens collected from 250-355 µm grain size fraction residues, with the exception of those from Sites 747 (>63 µm), 757

https://doi.org/10.5194/essd-2026-697
Preprint. Discussion started: 18 September 2026

Open Access Earth System Science Data Discussions

(250-425 μm), and 926 (150-355 μm). We did not apply any size correction to benthic foraminiferal Mg/Ca records, since, unlike their planktic counterparts, benthic foraminifera do not migrate in the water column during their life cycle. Therefore, they do not present significant Mg/Ca variability throughout their ontogeny (i.e., among different specimen sizes).

2.6 Converting Mg/Ca to temperature

2.6.1 Mg/Ca_{sw} reconstruction

To generate an updated record of temporal changes in Mg/Ca_{sw} through the Miocene, we compiled and reviewed existing proxy-derived Mg/Ca_{sw} estimates from the Oligocene through Modern (Appendix B: Fig. B1). The compilation, which includes estimates of Mg/Ca_{sw}, ages and uncertainties derived from halite fluid inclusions (Brennan et al. 2013; Horita et al. 2002; Lowenstein et al. 2001), calcium carbonate veins (CCVs; Coggon et al. 2010; Rausch et al. 2013), large benthic foraminifera (LBF; Evans et al. 2018), and echinoderm ossicles (Dickson, 2002; 2004), is largely based on the compilation of Tierney et al. (2019). We opted to omit the coral data (Gothmann et al. 2015), since they exhibit a high degree of scatter and their signal is unlikely to solely reflect changes to global Mg/Ca_{sw} (Lebrato et al. 2020). We expanded the compilation to include foraminiferal Na/Ca values, which were used to estimate past seawater [Ca^{2+}] (Zhou et al., 2021) and combined with [Mg^{2+}] measurements from halite fluid inclusions to estimate Mg/Ca_{sw} at a high resolution over the last 16 Myrs. Eight of the ten sites used in the Na/Ca record were key sites with updated MioOcean age models (DSDP 608 and 667; ODP 806, 925, 926, 1237, 1264; Integrated ODP U1337. The two remaining sites (ODP 758 and 807), which make up only 12 data points spanning the middle Miocene to Pleistocene, were not part of the MioOcean age model update, and published ages were used. Due to the high temporal resolution of the age models, the Na/Ca records do not have reported age uncertainties. We use the reported ages and uncertainties for all other Mg/Ca_{sw} proxy records listed above. The Modern Mg/Ca_{sw} was constrained using both observed (Broecker & Peng, 1982) and calculated (Lebrato et al. 2020) values.

We utilized a Monte Carlo approach to reconstruct Mg/Ca_{sw} from 34 Ma to present, resampling for uncertainties in age and propagating uncertainties in proxy values. We first generated 50,000 realizations of the input compilation, since many of the Mg/Ca_{sw} estimates have large age uncertainties. For each iteration, ages were randomly drawn from a uniform distribution bounded by the reported minimum and maximum ages for each respective data point. We also incorporated Mg/Ca_{sw} estimated from Na/Ca-derived Ca^{2+} values and independent Mg^{2+} concentration data. Mg^{2+} concentrations were randomly sampled from a uniform distribution of their reported age uncertainties and then interpolated to the ages of the Na/Ca-derived Ca^{2+} estimates. These paired Mg^{2+} and Ca^{2+} concentrations were used to determine Mg/Ca_{sw}, with uncertainty propagated from the Na/Ca-derived Ca^{2+} values. This process generated an ensemble of 50,000 possible input dataset that accounts for age uncertainty.

Each realization of the compilation was then converted into a 1.0-Myr binned reconstruction. Mg/Ca_{sw} values within each time bin were combined using inverse-variance weighting, and a representative value was randomly sampled from the resulting distribution. Finally, we generated a continuous Mg/Ca_{sw} curve from the binned ensemble by iteratively (N = 1,000) fitting a LOESS regression to the binned ensemble using a 13-Myr smoothing window (i.e., the residence time of Mg in seawater).

This procedure generated an ensemble of 1,000 smoothed Mg/Ca_{sw} reconstructions at 1.0-Myr intervals, from which the median and various percentiles were calculated (Appendix B: Table B1). The MATLAB script to generate the Mg/Ca_{sw} curve and the full Mg/Ca_{sw} ensemble curve are available in the project GitHub repository.

2.6.2 Planktic calibrations

Because planktic foraminiferal Mg/Ca records include data from species that calcify across a range of depths within the upper several hundred metres of the water column, and as these depths are often uncertain or variable through space and time (Chaabane et al. 2026), we classify Mg/Ca

https://doi.org/10.5194/essd-2026-697
Preprint. Discussion started: 18 September 2026

records as indicators of upper ocean temperature (UOT), rather than sea surface temperature (SST). This approach is consistent with the wider MioOcean effort (Sosdian et al. this volume).

To convert Mg/Ca to temperature, we applied two mutli-variable calibrations: the culture-derived calibration from Gray and Evans (2019; referred to hereafter as GE19) and the core-top/culture calibration from Tierney et al. (2019; referred to hereafter as BAYMAG). Both studies provide calibration frameworks that account for temperature, salinity, and seawater pH, with species-specific and pooled calibrations. The planktic Mg/Ca records in our Miocene compilation are derived from modern, extant morphotypes, and extinct species. Among these, some species are pH-insensitive, meaning their test Mg/Ca ratios are not significantly affected by seawater pH (e.g., *T. sacculifer*), whereas pH-sensitive species exhibit changes in test Mg/Ca as seawater pH varies (e.g., *G. bulloides, G. ruber*). For some extinct species, pH sensitivity remains poorly constrained (e.g., *D. altispira, G. obliquus*), whereas others have evidence for pH sensitivity or a close modern analogue based on comparisons with other species (e.g., *G. pseudopraebulloides*: Andersen et al., 2024; *G. subquadratus*: Boscolo-Galazzo et al., 2025).

Our high-confidence UOT estimates come from the pH-insensitive *T. sacculifer* group, including *T. sacculifer*, *T. trilobus*, and *T. quadrilobatus*. We treat *T. trilobus* and *T. quadrilobatus* as pH-insensitive based on their inclusion within the *T. sacculifer* plexus (Spezzaferri et al., 2015). We also calculate medium confidence UOT estimates from the pH-sensitive species: *G. bulloides.* Our lowest confidence UOT estimates come from the extinct species where pH sensitivity is unknown or poorly constrained*: G. praebulloides*, *D. altispira, G. obliquus, G. subquadratus*. Although available studies provide some constraints on pH sensitivity for *G. pseudopraebulloides* and *G. subquadratus*, these estimates remain low confidence. Note for *G. subquadratus*, we provide both taxon-specific and pooled calibration estimates, with taxon-specific estimates based on the *G. ruber* analogue; these results are reported in the Supplementary Table S3-S5.

The GE19 calibration equations follow the generalised equation:

$$Mg/Ca_{foram} = exp(a \times (S - 35) + b \times T + c \times (pH - 8) + d \quad \text{Eq. (2)}$$

, where *S* is salinity, *T* is temperature, *pH* is the seawater pH, *a, b,* and *c* are constants that reflect the sensitivity to each of those parameters, respectively*,* and *d* is the intercept term. Table 1 shows the corresponding *a*, *b*, and *c*, and values for each calibration used. For GE19, we use the 'generic' species equation for extant species and the multi-species equation for extinct species, except for *G. subquadratus*, for which we additionally apply the *G. ruber* species-specific calibration. It should be noted that Gray and Evans (2019) caution that the multi-species equation should only be used to reconstruct relative temperature changes. For pH-insensitive taxa, *c* is equal to zero, effectively removing the pH term. We rearrange this equation to solve for T and add a Mg/Ca_{sw} term to permit application of the calibration in deep time:

$$T = \left[ln\left(\frac{Mg/Ca_{foram}}{\Delta Mg/Ca_{sw}}\right) - d - a \times (S - 35) - c \times (pH - 8)\right] \times b^{-1} \quad \text{Eq. (3)}$$

, where $\Delta Mg/Ca_{sw}$ is the change in Mg/Ca_{sw} relative to modern [$(Mg/Ca_{sw})_{modern}$], and also accounting for the relationship between Mg/Ca_{sw} and Mg/Ca in foraminiferal calcite (*H*), such that the $\Delta Mg/Ca_{sw}$ at any particular time in the past [$(Mg/Ca_{sw})_{paleo}$] can be calculated as follows:

$$\Delta Mg/Ca_{sw} = \left[\frac{(Mg/Ca_{sw})_{paleo}}{(Mg/Ca_{sw})_{modern}}\right]^H \quad \text{Eq. (4).}$$

https://doi.org/10.5194/essd-2026-697
Preprint. Discussion started: 18 September 2026

Open Access Earth System Science Data Discussions

Table 1 Input parameters for UOT and BWT calculations, including calibration type, equation variables, and *H*-value. Uncertainty values are reported as 1 sigma. *Note GE19 follow the equation format as follows: Mg/Ca = exp(a×(S-35) + b×T + c×(pH-8) + d). **Note benthic calibration equation follows the format: Mg/Ca = a x exp$^{(b*T)}$

Planktic	Species	Calibration	Equation variables*							
			a	1σ	b	1σ	c	1σ	H	1σ
pH insens	*T. trilobus; T. sacculifer; T. quadrilobatus*	'Generic' species GE19	0.036	0.006	0.061	0.005	0.000	0.084	0.636	0.013
		Species-specific BAYMAG	Bayesian Mg/Ca calibration model						0.636	0.013
pH sens	*G. bulloides*	'Generic' species GE19	0.036	0.006	0.061	0.005	-0.877	0.121	0.636	0.013
		Species-specific BAYMAG	Bayesian Mg/Ca calibration model						0.636	0.013
extinct	*D. altispira; G. obliquus; G. subquadratus; G. psuedopraebulloides*	Multi'-species GE19	0.036	0.006	0.061	0.005	0.000	0.072	0.636	0.013
		Multi'-species GE19 (pH corr)	0.036	0.006	0.061	0.005	-0.73	0.072	0.636	0.013
		Pooled annual BAYMAG	Bayesian Mg/Ca calibration model						0.636	0.013
Benthic	**Species**	**Calibration**	**Equation variables****							
Infaunal	*O. umbonatus*	MioOcean (1)	0.480	0.118	0.090	0.003			0.609	0.152
		MioOcean (2)	0.329	0.149	0.114	0.020			0.838	0.204
		Lear et al. 2015	0.660	0.080	0.114	0.020			0.270	0.060
Epifaunal	*C. wuellerstorfi*	MioOcean	0.33	0.009	0.158	0.008			0.636	0.013

For each Mg/Ca observation, we calculated a 1,000 member ensemble of UOT values by simultaneously propagating uncertainties in Mg/Ca_{sw}, pH, *H*, and terms *a*, *b*, *c*, and *d*. While salinity almost certainly varied across the Miocene, there is not currently a reliable record of its temporal variability. Previous sensitivity analysis showed that temperatures calculated using salinity scenarios such as ± 1 psu modern salinity fall within the uncertainty envelope of the temperature calibration (Sosdian & Lear, 2020), indicating that minor changes in salinity will have a negligible impact on the UOT calculations. As there is currently no reliable and widespread proxy for paleosalinity, we use the modern sea surface salinity values for each site, extracted from the World Ocean Atlas 2013 version 2 (Boyer et al. 2013; Tierney et al. 2019), and do not account for uncertainties in this parameter. For each Mg/Ca value, we generated an ensemble of 1,000 Mg/Ca_{sw} values by linearly interpolating our smoothed Mg/Ca_{sw} ensemble to the age of the data. Likewise, to account for changes in pH across

https://doi.org/10.5194/essd-2026-697
Preprint. Discussion started: 18 September 2026

the Miocene, we used the percentiles reported in the recently compiled boron isotope-derived pH record from Whiteford et al. (2024) to develop a 1,000 member ensemble of possible pH values through time, which were then linearly interpolated to the age of each data point. We generated a 1,000 member ensemble of possible *H*-values from the normal distribution: *H ~ N(0.636, 0.013)* (Boscolo-Galazzo et al. 2025), and 1,000 member ensembles of each of the *a*, *b*, *c* terms by creating normal distributions using the mean and 1σ values reported in Table 1. The estimate of *H* is based on a compilation of calibration data spanning three planktic foraminiferal species and inorganic calcite (Mucci and Morse, 1983; Evans et al., 2015, 2016b; Holland et al., 2020; Boscolo-Galazzo et al. 2025) and represents a synthesis across multiple species. It is worth noting that Gray & Evans (2019) present two sets of species-specific calibrations: one where all four terms (*a*, *b*, *c*, and *d*) were solved for the regression, and a 'generic' calibration where the salinity (*a*) and temperature (*b*) constants were assumed/prescribed and only the pH (*c*) and intercept (*d*) terms were solved.

Here, we have opted to use the 'generic' temperature and salinity calibration equations for each species, as this significantly reduces the uncertainties of the temperature calculation (Gray & Evans, 2019). Additionally, the planktic Mg/Ca records utilised here were generated using different cleaning protocols (i.e., oxidative with or without reductive; Table A1). Reductive cleaning has been shown to lower Mg/Ca by ~10% (Barker et al. 2003; Rosenthal et al. 2004; Johnstone et al. 2016), although a study of a small subset of *T. trilobus* samples in the Late Miocene shows no clear offset in Mg/Ca when samples were subjected to oxidative-only vs oxidative-reductive cleaning (Martinot et al., 2022). Because the GE19 calibration is based solely on oxidatively cleaned culture data, we applied a cleaning correction to reductively cleaned samples by dividing their proxy values by 0.9. For samples in which the cleaning method was not specified, we assumed a cleaning effect halfway between oxidative-only and oxidative-reductive methods by dividing proxy values by 0.95. BAYMAG uses a set of Bayesian inverse models to predict UOT. A full explanation of the approach can be found in Tierney et al. (2019). Specifically for BAYMAG, we use the 'species' specific equation for extant species and 'pooled annual' equation for extinct species, except for *G. subquadratus*, for which we additionally apply the *G. ruber* species-specific calibration. Briefly, similar to GE19, the BAYMAG calibration includes species-specific models (Table 1) that account for temperature, salinity, and seawater pH; however, BAYMAG also includes a built-in cleaning correction (*clean*) and a carbonate dissolution correction, with the forward models following the generalised equation:

$$ln\left(Mg/Ca_{foram}\right) = \alpha + T \cdot \beta_T + S \cdot \beta_S + pH \cdot \beta_P + \Omega^{-2} \cdot \beta_O + (1 - clean \cdot \beta_C) + \epsilon + \left[\frac{(Mg/Ca_{sw})_{paleo}}{(Mg/Ca_{sw})_{modern}}\right]^H$$

Eq. (5)

Where β_T, β_S, β_P, β_O, and β_C are constants that reflect the sensitivity to temperature, salinity, pH, Ω, and cleaning method, respectively. α is the intercept term, and ϵ is the vector of residual errors. The dissolution correction utilises site-specific bottom water carbonate saturation state values (Ω). While evidence exists for episodes of widespread carbonate dissolution during the Miocene (e.g., the Carbonate Crash, Middle Miocene hyperthermals, MCO onset; Kochhann et al., 2016; Lübbers et al., 2019), site-specific dissolution histories remain poorly constrained, therefore, we consider two scenarios: one where we use the modern Ω value, extracted from GLODAPv2 (Lauvset et al. 2016; Tierney et al., 2019), and a second where we assume an Ω of 5, which implicitly assumes that there has been no dissolution (Tierney et al. 2019), rendering the correction negligible in the calculation of UOT. While the original version of BAYMAG assumed a linear relationship between Mg/Ca_{sw} and Mg/Ca in foraminiferal calcite (i.e., *H* = 1), the model has subsequently been updated to allow users to input their own *H*-values, which we further modified to accept a vector rather than a scalar *H* input. By its nature, BAYMAG also uses an ensemble approach, sampling from uncertainties in the Mg/Ca_{sw} values and calibration terms. As with the GE19 calculation, we used the modern site-specific salinity values; however, in an effort to minimise computational expense, we opted to use the median paleo-pH value for each data point, rather than the full ensemble. The UOT ensembles were calculated using a prior standard deviation of 7.5°C, and we modified the MATLAB function to use our new Mg/Ca_{sw} curve, rather than the built-in reconstructions.

https://doi.org/10.5194/essd-2026-697
Preprint. Discussion started: 18 September 2026

Open Access Earth System Science Data Discussions

In total we have produced three UOT calibration scenarios: (1) GE19, (2) BAYMAG, assuming the modern Ω value, and (3) BAYMAG, assuming an Ω value of 5. We compare these scenarios in Section 3.4. Note that BAYMAG temperature estimates are only calculated when at least two Mg/Ca measurements are available for a site. Separate files containing 2.5th, 16th, 50th, 84th, and 97.5th percentiles of the UOT values can be found in the MioOcean database (Sosdian et al. this volume) and is openly accessible and can be downloaded directly through the MioOcean website at https://www.miocean.com/download-data/ or through Zenodo (https://doi.org/10.5281/zenodo.22258386, Sosdian et al. 2026). The code to reproduce the UOT calculations can be found in the Mg/Ca MioOcean GitHub repository.

2.6.3 Benthic calibrations

As with data from planktic foraminifera, we use species-specific calibrations to calculate BWT from the benthic foraminifera Mg/Ca compilation. Here, we focus on generating high-confidence temperature estimates from records from shallow infaunal *O. umbonatus and* medium-confidence from the epifaunal *C. wuellerstorfi*. Both species are extant and cosmopolitan. The benthic Mg/Ca calibrations applied here follow the generalized equation:

$$Mg/Ca_{foram} = A \times Mg/Ca_{sw}{}^{H} \times exp(B \times T) \qquad \text{Eq. (6)}$$

, where *A* and *B* are constants, reflecting the sensitivities to Mg/Ca_{sw} and temperature, respectively. Recent multivariate global core top calibrations including BWT and Ω from Nauter-Alves et al. (2025) demonstrated a significant temperature sensitivity for *O. umbonatus* Mg/Ca, whereas they note a limited sensitivity for *C. wuellerstorfi* Mg/Ca, with a significant component related to saturation state for this species. These calibrations include input parameters to convert Mg/Ca to temperature including saturation states histories derived from Sr or B or Mg/Li records from companion species or archives. We do not adopt the calibrations presented in Nauter-Alves et al. (2025) as there are limited records of carbonate chemistry histories in the past to accurately reconstruct this variability. However, we do modify the core-top data that underpin the *C. wuellerstorfi* calibration used here to minimize the impact of saturation state (see below). Ultimately, we compare our infaunal and epifaunal Mg/Ca-derived temperature results (see section 3.3.2) from ODP Site 806 with Nauter-Alves et al. (2025) calibration estimates, providing support for our medium and high-confidence BWT records.

We calculated BWTs from Mg/Ca ratios of *O. umbonatus* by following the calibration framework of Lear et al. (2015) which uses estimate of seawater Mg/Ca and BWT for the modern and ice-free Paleocene to constrain calibration parameters *A* and *H*. The Lear et al. (2015) calibration uses the temperature sensitivity (*B* in equation 3) of 0.114 from the core top calibration of Lear et al. (2002). The Paleocene bottom water temperature used in that calculation was derived from benthic foraminiferal $\delta^{18}O$ assuming ice free conditions. However, recent work using clumped isotopes has raised the possibility of variable $\delta^{18}O_{sw}$ in the ice free world of the early Paleogene (Meckler et al., 2022). Therefore, we recalculated the values of A and *H* using clumped isotope temperatures for the Paleocene, following the general approach of Lear et al. (2015) while propagating uncertainty in all terms, assuming two scenarios referred as: MioOcean calibration (1) a Mg/Ca-temperature sensitivity of 0.09 from Anand et al. (2003) and MioOcean calibration (2) using temperature sensitivity of 0.114 from Lear et al. et al. (2002) (Table 1).

For the ice-free Paleocene, we used clumped-derived BWT (Agterhuis et al., 2022; Meckler et al., 2022), *O. umbonatus* Mg/Ca measured at 54.1 Ma at ODP Site 690 (Lear et al., 2015), and Mg/Ca_{sw} estimates from Evans et al. (2018). For the modern ocean, we extracted BWT from GLODAP for the location of ODP Site 806, which was paired with the oxidatively cleaned core-top *C. wuellerstorfi* at ODP Site 806 (Billups and Schrag, 2003). We multiplied the value by 0.9 to account for the cleaning method and by 1.19 to account for the observed interspecific offset between *C. wuellerstorfi* and *O. umbonatus* at ODP Site 806 (Lear et al., 2003), and assigned a 1% relative uncertainty, effectively deriving a synthetic modern *O. umbonatus* dataset. We created 1,000-member ensembles for each input parameter used in the calibration, drawing from a normal distribution

https://doi.org/10.5194/essd-2026-697
Preprint. Discussion started: 18 September 2026

defined by the specified mean and 1σ of each value, and used the smoothed ensemble curve values at 0.0 Myr for modern Mg/Ca_{sw}. We then propagated these ensembles through the calibration to produce 1,000-member ensembles of *A, B,* and *H*.

For MioOcean calibration 1 we note that this new calibration assumes a generic temperature sensitivity (i.e., *B*=0.09; Anand et al. 2003) which produces a value of *H* (0.603), similar to the planktic Mg/Ca-temperature calibrations described above. For MioOcean calibration 2, we use B=0.114 (Lear et al. 2002), producing a H value of 0.838. Core-top calibrations for *O. umbonatus* used reductive cleaning and, as all downcore data was generated using a similar approach, no cleaning correction was applied to our compiled downcore records (Table A2). We compare and evaluate these *O. umbonatus* calibrations in section 3.3.2

For each Mg/Ca observation, we calculated a 1,000-member ensemble of BWT by simultaneously propagating uncertainties in the calibration parameters and Mg/Ca_{sw}. For these calculations, each ensemble value used paired *A, B,* and *H* values from the calibration ensemble, preserving their interdependence and Mg/Ca_{sw} was linearly interpolated from the smoothed ensemble curve to the age of each observation. We note that some uncertainties are impossible to quantify, e.g., unknown evolutionary changes in vital effects through time.

We developed a new calibration for the epifaunal *C. wuellerstorfi* using the coretop compilation of Lo Giudice Capelli et al. (2015). We excluded (1) data from cold, undersaturated waters, due to carbonate ion saturation state effects at the low- and high-temperature ends of calibrations (Lear et al. 2002; Elderfield et al. 2006; Yu & Elderfield, 2008; Lo Giudice Capelli et al. 2015), and (2) data from supersaturated (i.e., >80 μmol/kg) waters in the northwestern Pacific, since they have been shown to cause Mg depletion in foraminiferal shells (Kubota et al., 2015). We fit the remaining data with an exponential curve relating temperature to foraminiferal Mg/Ca, and generated a 1,000-member ensemble of *B* values sampled from a normal distribution defined by the fitted coefficient value and its uncertainty. Likewise, we generated an ensemble of 1,000 possible *H*-values using the values reported by Boscolo-Galazzo et al. (2025; 0.636 ± 0.013). For each paired *B* and *H* value, we calculated *A* from each core-top Mg/Ca and temperature observation using the calibration equation and took the median across the core-top observations to obtain the corresponding *A* value. The mean and 1σ values of *A*, *B*, and *H* for the *C. wuellerstorfi* calibration can be found in Table 1, and the full ensemble files and code to reproduce the calibration can be found in the Mg/Ca MioOcean GitHub repository.

All of the core-top data used in the calibration were reductively cleaned. Some studies suggest that, similar to planktic foraminifera, this method reduces the measured Mg/Ca values in benthic foraminifera by 10% (Yu et al. 2007). Other studies have shown no significant offset between Mg/Ca values from samples with and without reducing cleaning in *O. umbonatus* and *C. wuellerstorfi* (Lear et al. 2003; Nauter-Alves et al., 2025). This builds on the work of Martin & Lea (2002) which shows the offset might be species and site specific. In line with the planktics and previous work, we corrected the data cleaned only with oxidative methods by multiplying their values by 0.90 to bring them in-line with the calibration, and we adjusted samples for which the cleaning method was not specified by multiplying their values by 0.95. We provide both the corrected and uncorrected BWT datasets as part of the MioMG output.

To calculate BWT from *C. wuellerstorfi* Mg/Ca values, we rearranged Eq.6 to solve for temperature:

$$T = B^{-1} \times ln\left(\frac{Mg/Ca_{foram}}{A \times Mg/Ca_{sw}{}^{H}}\right) \qquad \text{Eq. (7).}$$

For each Mg/Ca observation, we calculated a 1,000 member ensemble of BWT values by simultaneously propagating uncertainties in A, *B*, *H*, and $Mg/Ca_{sw.}$ Each ensemble member used a matched set of *A*, *B*, and *H* values, preserving the dependence of *A* on *B* and *H* that was established during the calibration. Mg/Ca_{sw} was linearly interpolated from the smoothed ensemble to the age of the data.

https://doi.org/10.5194/essd-2026-697
Preprint. Discussion started: 18 September 2026

Open Access Earth System Science Data Discussions

For the *C. wuellerstorfi* calibration, as noted above and outlined in Nauter-Alves et al. (2025), there is additional uncertainty related to carbonate saturation state. *Cibicidoides wuellerstorfi* Mg/Ca has been estimated to have a Mg/Ca-CO_3^{2-} sensitivity of 0.0086 mmol/mol per µmol/kg, but only up to a threshold of 25 µmol/kg, above which the carbonate saturation state effect is negligible (Elderfield et al. 2006; Nauter-Alves et al. 2025). Because Miocene bottom-water carbonate saturation state is not well constrained at individual sites, we do not include this potential effect in our reported uncertainties; therefore, Mg/Ca-based BWT estimates from deeper sites, such as ODP Site 926 (3598 m), should be interpreted with caution as they may carry additional uncertainty associated with carbonate undersaturation.

Files containing 2.5th, 16th, 50th, 84th, and 97.5th percentiles of the BWT values can be found in the MioOcean database (Sosdian et al. submitted) and can be downloaded directly through the through the MioOcean website at https://www.mioocean.com/download-data/ or through Zenodo (https://doi.org/10.5281/zenodo.22258386, Sosdian et al. 2026). The code to reproduce the BWT calculations can be accessed through the Mg/Ca MioOcean GitHub repository.

2.7 Interactive data visualisation

To allow specialists and non-specialists to explore the MioOcean Mg/Ca compilation easily and provide a portal for data examination and visualization, we generated a Python-based Streamlit dashboard: https://mio-mg.streamlit.app, which can also be accessed directly through the MioOcean website https://mioocean.com/temperature-proxies/mg-ca/. The dashboard allows the users to explore Miocene Mg/Ca-derived UOT and BWT data interactively including site inspection of location, data density, paleo-coordinates, and underpinning published or MioOcean age model. Further, users can apply proxy-specific filters to explore the data in categories such as ocean region or latitudinal, species, size fraction, and foraminiferal cleaning method. Interactive calibration function allows researchers to interrogate a range of approaches used to convert Mg/Ca to temperature and facilitate meaningful interpretations. The Streamlit dashboard is directly connected to the most recent uploaded data compilation files published on Zenodo (https://doi.org/10.5281/zenodo.22258386, Sosdian et al. 2026) and can be continuously updated and adjusted based on the user's needs. More information on the data management and storage can be found in the MioOcean database paper (Sosdian et al. submitted).

3. Results & Discussion

3.1 Compilation of Mg/Ca_{sw}

The compiled MioOcean Mg/Ca_{sw} curve (Figure 3), presented here, derives from halite fluid inclusions, CCVs, LBF, echinoderm ossicles, and Na/Ca records, including updated ages for key Na/Ca site records. MioOcean Mg/Ca_{sw} increases from values of ~2 mol/mol during the MCO to a modern value of 5.2 mol/mol (Broecker & Peng, 1982; Ries, 2001). Although the average modern Mg/Ca_{sw} is 5.2 mol/mol, recent studies (Lebrato et al. 2020) have shown variations in Mg/Ca_{sw} across ocean regions of similar magnitude to changes in the Neogene. The uncertainty envelope for the MioOcean Mg/Ca_{sw} compilation is relatively large in the Oligocene, due to sparse data coverage and proxy-specific uncertainties but narrows through the Miocene toward the present. We therefore designate the Miocene portion of the record as high confidence where data coverage and agreement among records provide greater confidence in the reconstructed Mg/Ca_{sw} evolution.

Previous studies have compiled Mg/Ca_{sw} records (Tierney et al. 2019; Sosdian & Lear, 2020; Rosenthal et al. 2022; Evans et al. 2026) using a varying set of proxy archives. The BAYMAG compilation (Tierney et al. 2019) is largely similar to the one presented here; however, it includes coral data and excludes the Na/Ca data. The smoothed curves are within error of one another during the Early Miocene. However, they diverge in the Middle Miocene (~16 Ma), coinciding with the start of the NaCa-derived data, with the MioOcean Mg/Ca_{sw} record indicating lower values (by ~1 mol/mol) and different trajectory than those shown in the BAYMAG curve (Fig. C1; Tierney et al., 2019). Sosdian & Lear. (2020) used the BAYMAG approach however omitted coral data due to scatter and non-thermal controls as highlighted above (Fig. C1). Recently, Rosenthal et al. (2022) combined

https://doi.org/10.5194/essd-2026-697
Preprint. Discussion started: 18 September 2026

foraminiferal derived Neogene Na/Ca data along with halite fluid inclusion data to reconstruct Mg/Ca$_{sw}$ variations, and Evans et al. (2026) expanded this compilation by incorporating additional foraminiferal Na/Ca records along with inclusion data from the Plio-Pleistocene and Paleogene as well (Fig. C1). The MioOcean Mg/Ca$_{sw}$ curve is broadly consistent with Sosdian & Lear (2020), Rosenthal et al. (2022), and Evans et al. (2026). Recent online updates from BAYMAG (2026) provide 2 Mg/Ca$_{sw}$ options as follows: (1) echinoderm ossicles, LBF, CCV, halite fluid inclusions, and coral and (2) echinoderm ossicles, LBF, CCV, halite fluid inclusions, and Na/Ca.

Our new Mg/Ca$_{sw}$ curve also matches well in terms of absolute values and trends with the MgCa$_{sw}$ reconstruction Higgins & Schrag (2015), based on records of the Mg isotopic composition of pelagic carbonates and associated pore fluids and box modelling (Fig. C1). Within model scenarios, the Higgins & Schrag (2015) curve is intermediate in terms of relative change since the Miocene (Hardie, 1996; Higgins & Schrag 2012, Fante & DePaolo 2006) (Fig. C1). Overall, we suggest that, moving forward, the MioOcean Mg/Ca$_{sw}$ compilation, which uses a suite of independent Mg/Ca$_{sw}$ estimates from a range of proxies should be used in Mg/Ca paleothermometry across the Miocene. In the future, higher resolution robust archives of seawater chemistry should reduce the uncertainty associated with temperature estimates on geological timescales.

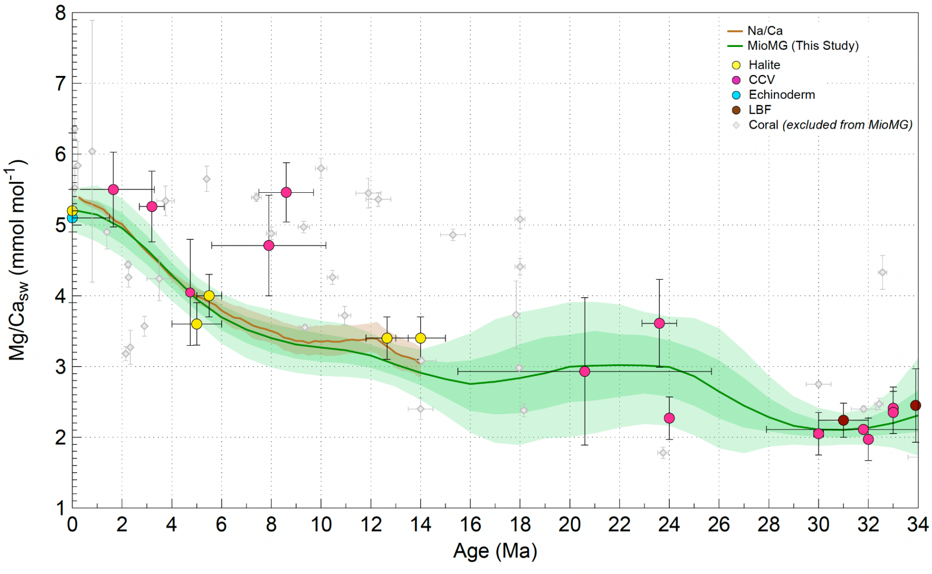

Figure 3. MioOcean Mg/Ca$_{sw}$ reconstruction for the Miocene (MioMG). Mg/Ca$_{sw}$ proxy reconstructions derive from a range of approaches including halite fluid inclusions, calcium carbonate veins (CCV), corals, echinoderm ossicles, large benthic foraminifera (LBF), and foraminiferal Na/Ca values combined with [Mg^{2+}] measurements from halite fluid inclusions (Lowenstein et al. 2001; Horita et al. 2002; Dickson, 2002, 2004; Brennan et al. 2013; Coggon et al. 2010; Rausch et al. 2013; Gothmann et al. 2015; Evans et al. 2018; Zhou et al., 2021). Note the Mg/Ca$_{sw}$ data derived from corals (Gothmann et al. 2015) exhibit a high degree of scatter and were therefore omitted from the compilation. Uncertainties in age and proxy value are included for each record.

3.2 Preservation assessment

To document foraminiferal preservation, we considered the range of approaches used across the legacy of the Ocean Drilling Program. Traditional approaches to assessing preservation include use of scanning electron microscopy (SEM) images and light microscopy (LM). In earlier studies, images from a single foraminiferal test were used to represent the study interval. This contrasts with

https://doi.org/10.5194/essd-2026-697
Preprint. Discussion started: 18 September 2026

recent approaches using multiple images from the test to wall scale across multiple depth intervals to identify excellent to poor preservation through time (Sexton et al., 2006; Pearson and Burgess, 2008; Sexton and Wilson, 2009; Edgar et al., 2013; Edgar et al., 2015; Rosenthal et al., 2018). Regardless of approach, estimating the quantitative effect that diagenetic alteration, identified by these visual approaches, has on Mg/Ca values adds another layer of complexity.

Dissolution can be identified by binocular microscopy and SEM, but quantifying its impact on Mg/Ca is not possible with these standard imaging techniques. It has been shown to reduce planktic Mg/Ca, though evidence is less clear for benthic Mg/Ca (Dekens et al., 2002, Lear et al., 2010; Rongstad et al., 2017; Mawbey and Lear, 2013).

Authigenic coatings usually have higher Mg/Ca values than the foraminiferal test, but the magnitude of the effect on measured Mg/Ca is strongly dependent on the [Mg^{2+}] of the coating. Authigenic coatings made of calcite cements are evident from SEM, but oxides are more difficult to identify using standard SEM of whole test-images (Pena et al., 2005; Detlef et al., 2020). Identifying the exact coating requires the specimen to be cracked open and looked at with more advanced techniques such as backscatter electron microscopy, energy dispersive x-ray spectroscopy (EDS) or electron microprobe (EMPA) analysis (Pena et al., 2005; Detlef et al., 2020; Staudigel et al., 2022; John et al. 2023). Complementary trace metal records, such as Fe, Al, Ti, and Mn can aid in assessing the impact of authigenic overgrowths and diagenetic environment.

Recrystallization can be readily identified by SEM, but there is no clear relationship between recrystallization and geochemical alteration of Mg/Ca because it usually happens in closed-system conditions (Edgar et al., 2013, Staudigel et al., 2022). The geochemical impact is clearer for $\delta^{18}O$ in planktic foraminifera (Sexton et al., 2006), although research indicates that benthic $\delta^{18}O$ is not significantly affected, as any recrystallisation happens shortly after deposition in pore waters with an oxygen isotopic composition similar to deep water masses (Edgar et al., 2013). Interestingly, recent work has shown that despite some textural recrystallisation, planktic foraminifera maintain their intra-test Mg/Ca banding, supporting use for paleotemperature reconstructions (John et al. 2023).

For the MioOcean Mg/Ca compilation, we combined author and literature recommendation to adopt a publication-level preservation state, though we acknowledge that, frequently, these assessments are subjective. The overwhelming majority of compiled studies (90%; 35/39) report some information concerning specimen preservation state, with 64% (25/39) of the studies providing or referencing publications with images that document the preservation state (Supplementary Table S6; references cited herein). Of the studies where SEM or other images, such as LM or computed tomography (CT), are reported/referenced, 52% (13/25) use a single sample to represent the full study interval. Just over half the studies (56%; 22/39) list the specific criteria they used to determine the preservation state, and under a third of studies (31%; 12/39) utilise other evidence that can indicate preservation levels (such as Sr/Ca ratios or other non-Mg contaminant indicators). No mention of preservation state at all was rare (10%; 4/39). The typical approaches to identifying preservation include the visual assessment of preservation state using LM (sometimes mentioning specific criteria), referencing the site report, and/or providing (SEM) images to document species concept and specimen state. Recent Mg/Ca studies made more regular use of additional approaches to assess preservation state, for instance using advanced imaging (SEM, CT), documenting multiple samples and/or utilising additional proxies (e.g., Sr/Ca ratios etc). Use of advanced geochemical characterisation approaches, such as EMPA, to identify and quantify the impact of preservation, was not found within the MioOcean Mg/Ca datasets.

Overall, we see a range of preservation states reported, spanning moderately good preservation to excellent/enhanced foraminiferal preservation. Only one study reported moderate to poor preservation. Frequently, the authors reported that they intentionally selected well-preserved specimens with glassy tests, and often provided additional qualitative information describing the preservation state (e.g., no signs of dissolution, preservation of original features, presence of microrecrystallisation). We have collated multi-scale SEM images from several Miocene Mg/Ca studies including the compilation (ODP site 1146, Integrated ODP sites U1338 and U1443), which demonstrate how preservation can vary over space and time (Miocene to Pleistocene), including at

https://doi.org/10.5194/essd-2026-697
Preprint. Discussion started: 18 September 2026

the same location (Figure 4). This variation is not always straightforward to predict based on our understanding of the main drivers of preservation. While this overview is not an in-depth assessment, we highlight that preservation and the processes that control it at any individual study location are complex and variable.

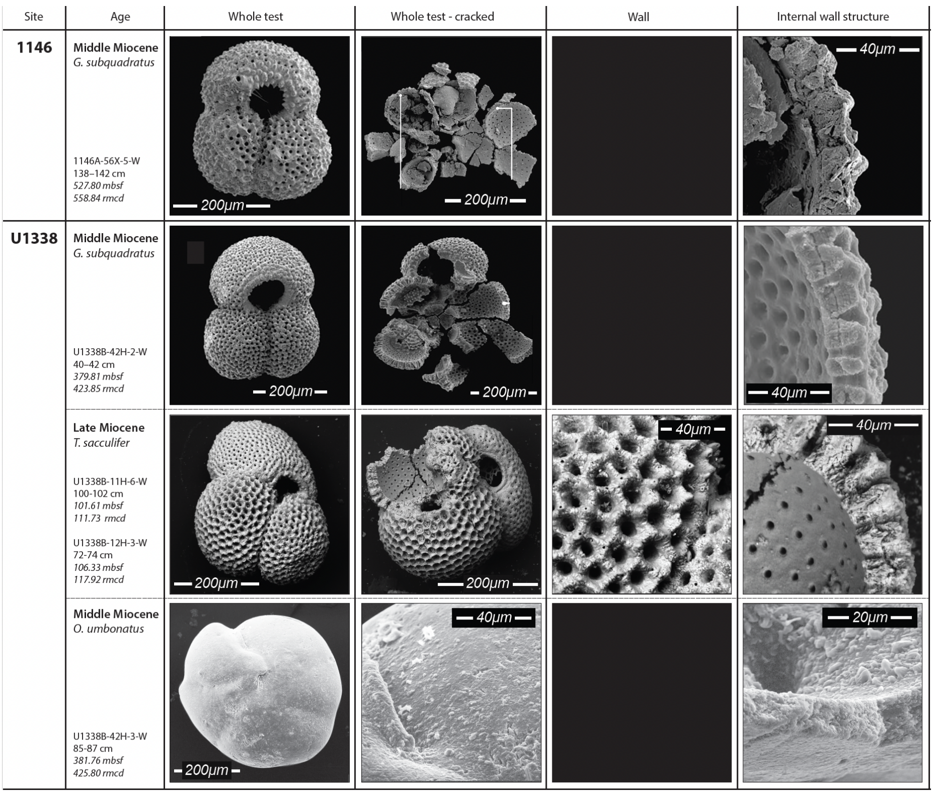

Figure 4. Multi-scale SEM images from several Mg/Ca studies incorporated into the MioOcean database, including ODP Site 1146 planktic records and IODP Site U1338 planktic and benthic foraminiferal records (Fox and Wade, 2013; Drury et al. 2014; Fox et al. 2021, Kochhann et al. 2017). Images show the variability in preservation across the foraminiferal test and throughout the Miocene.

Generally, the preservation shown in the SEM images aligns with the preservation state reported by the authors. Even though visual assessments are subjective and do not quantify the impact of the preservation state on Mg/Ca, it appears that the community selects specimens that generally fall in the fair-to-good (occasionally excellent) range (benchmarked against Appendix A; Fig. A1). None of the documented specimens (including those reported as "frosty" with microrecrystallisation) showed preservation as poor as the "poor" example(s) from International ODP Expedition 363 (Fig. B1). Overall, the scientific community endeavours to use well preserved material to limit the diagenetic impact on test Mg/Ca. Regarding the MioOcean Mg/Ca data, we conducted a thorough review of the available quantitative and qualitative preservation information. We found that in nearly all cases, our diagenetic assessment aligned well with screening protocols implemented by the original authors. We therefore treat the data as suitable for inclusion unless the original authors flagged the preservation state as problematic and indicated that it likely negatively impacted reported Mg/Ca values.

https://doi.org/10.5194/essd-2026-697
Preprint. Discussion started: 18 September 2026

Open Access Earth System Science Data Discussions

Going forward, we recommend a more in-depth temporal, multi-proxy view of preservation generating SEM images of multiple angles and scales (e.g., whole test, cracked test, outer wall zoom, inner wall zoom) at discrete time slices in the Miocene (Figure B1). Key examples of this approach are given in Sexton et al. (2006), Edgar et al. (2013) and Rosenthal et al. (2018) and provided in Fig. B1 (adapted from Rosenthal et al., 2018). We also suggest that preservation analysis via SEM or light microscopy should be paired with additional techniques that identify impacts on the Mg/Ca signal, whenever possible. This includes EMPA analysis of individual foraminifera across depth intervals to determine if primary Mg/Ca banding is maintained (Staudigel et al. 2022) and use of contamination indicators (Al, Fe, Mn) to denote different types of overgrowth.

3.3 Ocean temperature records

This section evaluates the Miocene UOT and BWT estimates generated using the MioMG framework and examines how different calibration choices and assumptions influence reconstructed temperatures.

3.3.1 Implications of UOT calibration scenarios

We compare MioMG-derived UOTs with previously published temperature estimates (Figure 5) focusing on a set of representative case studies spanning pH-insensitive, pH-sensitive, and extinct planktic foraminiferal species. These examples highlight the sensitivity of reconstructed temperatures to calibration choices and allow us to examine Miocene climate features. We also examine effects of incorporating updated Mg/Ca_{sw} composition, pH effects, and carbonate dissolution. Future evaluation of Mg/Ca-derived temperatures across the entirety of the Miocene is ongoing as part of the second phase of the MioOcean effort. Accordingly, in this section we focus on the MCO, representing warmer-than-modern conditions, and the subsequent cooling across the MMCT. We also highlight remaining uncertainties and priorities for future proxy development.

Previous approaches use either site-specific calibrations, generic planktic equations, or those with depth correction and variable approaches to accounting for changes in Mg/Ca_{sw} changes or *H*-value. The MioMG effort focused on equations that include multi-variable aspects due to recent knowledge of non-thermal controls deriving from core-top and sediment-trap data and culturing compilations. Using the GE19 and BAYMAG equations, we estimated temperature for a range of planktic species as outlined in 2.5.1. For all BAYMAG UOT estimates, we present two scenarios in the output, namely one with no dissolution correction (assuming an Ω of 5) and one with a dissolution correction (assuming a modern, site-specific Ω value). Due to the general lack of site-specific dissolution histories, we compare UOT estimates derived only from the BAYMAG scenario with no dissolution correction. This correction impacts UOT values significantly; for instance, dissolution-corrected BAYMAG UOT estimates from the MCO are significantly warmer (34°C) than uncorrected UOTs (32°C). Future work to constrain site-specific carbonate dissolution histories would allow for better constraint on the upper limit of MCO UOTs.

The tropical Atlantic ODP Site 926 Mg/Ca record (Sosdian et al. 2018, 2020) derives from the pH-insensitive species *T. trilobus* and spans the entirety of the Miocene (Figure 5a). Both MioOcean calibrations indicate that UOTs reached maximum values during the MCO (14.7-16.9 Ma) followed by long-term cooling through the remainder of the Miocene. Sosdian et al. (2018) calculated UOTs for Site 926 Mg/Ca using the *T. sacculifer* sediment trap calibration from Anand et al. (2003; 9% temperature sensitivity) with *H*-value of 0.41 (Delaney et al. 1985; Hasiuk & Lohmann, 2010) and Mg/Ca_{sw} value of 3.43 mol/mol based on fluid inclusion data (Horita et al. 2002; Brennan et al. 2013). Their MCO UOT estimates were 28°C, cooler than the MioOcean estimates derived here. This difference is primarily driven by lower MioOcean Mg/Ca_{sw} estimates used here for the MCO and the higher *H* value (Boscolo-Galazzo et al. 2025).

Southern Ocean ODP Site 1092 Mg/Ca record (Kuhnert et al. 2009) derives from the pH-sensitive species *G. bulloides* and covers the Middle Miocene climate transition (14.7 to 13.2 Ma) (Figure 5b). Both MioOcean calibrations indicate warmer UOTs prior to the MMCT followed by pronounced cooling across the MMCT. In comparison, the original calibration applied in Kuhnert et al. (2009) using a species-specific culture data (Mashiotta et al., 1999), with no Mg/Ca_{sw} correction,

https://doi.org/10.5194/essd-2026-697
Preprint. Discussion started: 18 September 2026

indicates a similar overall pattern but cooler pre-MMCT temperatures and a smaller magnitude MMCT cooling. These differences primarily reflect differences in the treatment of Mg/Ca$_{sw}$, *H*-value, and pH. In addition, as *G. bulloides* has been identified as a pH sensitive species, corrections for changes in pH across the MMCT have increased the magnitude of temperature change.

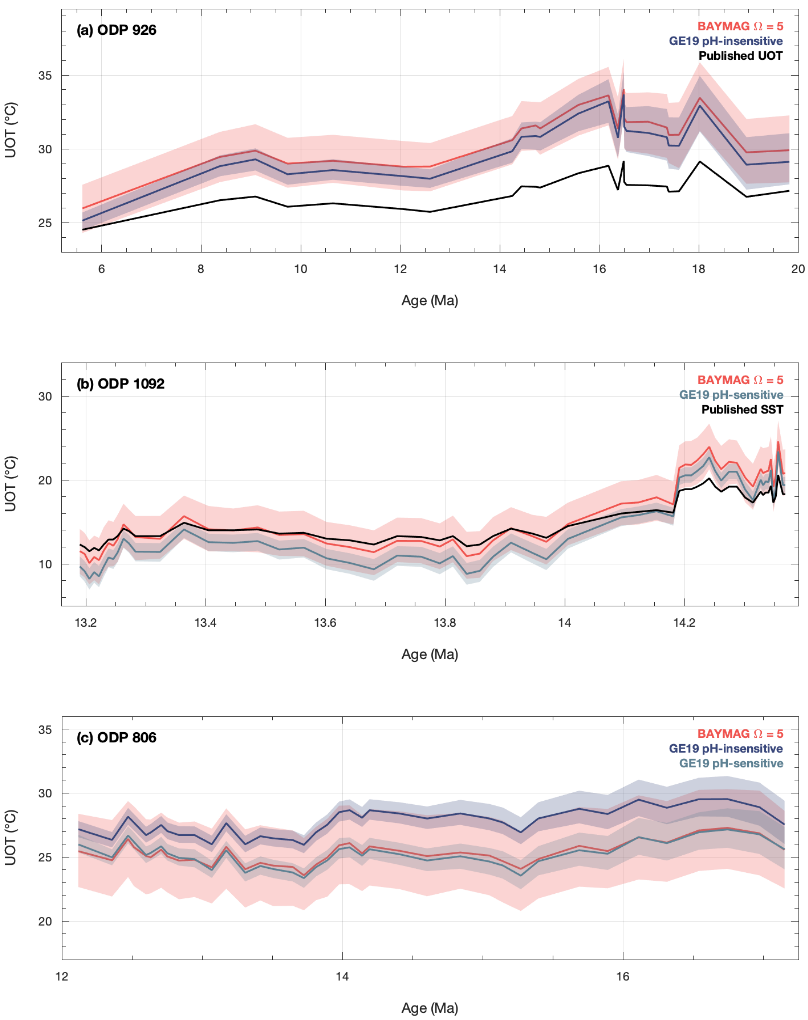

Figure 5. UOT scenarios derived from GE19 and BAYMAG calibrations for three planktic foraminifera from key sites. (a) ODP Site 926 Mg/Ca-UOT estimates from pH-insensitive *T. trilobus*, (b) ODP Site 1092 Mg/Ca-UOT estimates from pH-sensitive *G. bulloide*s, and (c) extinct *D. altispira* Mg/Ca-UOT estimates from ODP Site 806. 68% confidence level envelopes are shown. Published UOT estimates from Sosdian et al (2018) and Kuhnert et al. (2009) are shown in (a) and (b) for comparison. ODP site 806 published UOT estimates were reported as relative changes in UOT (Sosdian & Lear, 2020) and not included here for comparison. Note x-axis modified in each panel to showcase the full length of available records.

https://doi.org/10.5194/essd-2026-697
Preprint. Discussion started: 18 September 2026

Oceanic pH estimates are derived from a boron isotope derived compilation (Whitford et al. 2024) and show a MMCT change of 0.3 pH units. Moving forward, site-specific pH records are ideally needed to distinguish regional changes in pH associated with frontal changes and surface CO_2 variability from the global ocean pH evolution used here, as likely in ODP site 1092.

Western Pacific Warm Pool ODP Site 806 Mg/Ca record (Sosdian et al. 2020) derives from extinct species *D. altispira* and covers the interval 16.5 to 11.5 Ma (Figure 5c). As the pH sensitivity is unknown for *D. altispira*, we evaluate UOT estimates derived from both pH-corrected and uncorrected GE19 and pooled annual BAYMAG calibrations. Both calibrations indicate warmer UOTs during the MCO and cooling across the MMCT, although the magnitude of both the absolute temperatures and the cooling depends on the treatment of pH. Sosdian et al. (2020) applied the Anand et al. (2003) multi-species equation and compiled a Mg/Ca_{sw} polynomial equation with 3.8 mmol/mol value in MCO and *H* value of 0.41 and showed a 1.5°C cooling across MMCT, in line with pH-uncorrected scenarios above. This pattern is reproduced when reviewing the calculated UOTs from the ODP Site 845 *D. altispira* Mg/Ca record as well (Hess et al. 2023). However, because the MMCT coincides with substantial changes in oceanic pH (Sosdian et al. 2018), determining the magnitude of cooling from the MCO to the post-MMCT requires a better understanding of the pH sensitivity of *D. altispira*. Future work could include examining contemporaneous records of UOT and pH from the same site to pinpoint the role of non-thermal drivers of Mg/Ca variability in extinct Miocene species.

When considering the MioMG UOT product for the remaining sites, some sites stand out with higher mean Mg/Ca values relative to the Miocene Mg/Ca compilation. Sites RIP and ODP 872 have mean *T. trilobus* Mg/Ca of 4.70 mmol/mol, with UOT estimates suggesting significantly warmer-than-present conditions in the early Miocene and middle Miocene (Badger et al. 2013; Greenop et al. 2019; Sosdian et al. 2020; Boscolo-Galazzo et al. 2021). Additional multi-proxy reconstructions are needed from these sites to provide context on these warm UOT values.

Overall, Mg/Ca-derived UOTs showcase key features of the Miocene climate system, including warming during the MCO and cooling across the MMCT. Absolute UOT estimates have corresponding uncertainties such as 2.0-3.0°C at 68% confidence interval and 4.0-5.0°C at 95% CI. These are associated with uncertainty in input parameters including calibration, *H*-value, Mg/Ca_{sw}, and pH correction (if applied). Smaller uncertainties are associated with examining relative changes in UOT during periods when there are smaller changes in Mg/Ca_{sw} and pH (Late Miocene). An important advantage of this reconstruction is that these uncertainties are explicitly quantified, allowing UOT estimates from different sites, studies, and calibrations to be directly compared to one another. Reducing uncertainty in Middle Miocene UOT estimates requires additional work using multi-proxy reconstructions to delineate non-thermal factors and new proxies or additional records to determine absolute Miocene Mg/Ca_{sw} values with higher confidence and resolution.

3.3.2 Implications of BWT calibrations scenarios

We illustrate the results of the four BWT calibrations described in section 2.6.3 and compare the benthic foraminiferal Mg/Ca records from ODP Sites 806 and 926 (Figure 6). These Mg/Ca records were measured on both *O. umbonatus* and *C.* wuellerstorfi (Lear et al., 2003, 2015*)* and encompass markedly different water depths, and, therefore, different carbonate saturation states (2,521 m at Site 806; 3,598 m at Site 926).

https://doi.org/10.5194/essd-2026-697
Preprint. Discussion started: 18 September 2026

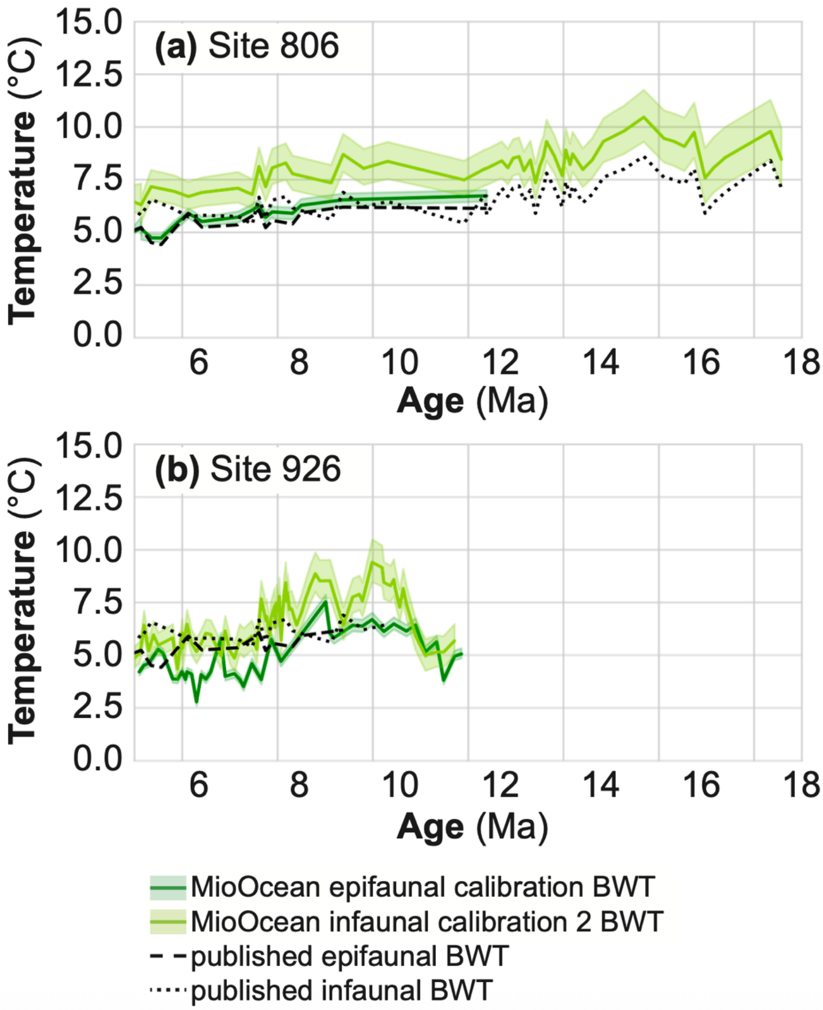

Figure 6. Comparison of BWT estimates from epifaunal (revised Lo Giudice Cappelli et al., 2015 calibration; dark green) and infaunal (MioOcean calibration 2; light green) species of benthic foraminifera at (a) ODP Site 806 and (b) ODP Site 926 with published BWT estimates. 68% confidence level envelopes are shown.

At Site 806, *O. umbonatus*-derived BWT were calculated using MioOcean calibration 2 (Table 1; *H*=0.838) and corrected for changes in Mg/Ca_{sw} using the new MioOcean compilation (Figure 6a). Average BWT was 9.6°C during the MCO (16.9-14.7 Ma), which is warmer than the average BWT of 7.4°C originally reported by Lear et al. (2015) for the same interval. The new MioOcean calibration 1 yields comparable average BWT for the MCO of 9.9°C (Table 1; *H*=0.609), and the Lear et al. (2015) calibration (Table 1; *H* =0.27) yields a colder average BWT of 7.9°C (Appendix C: Fig. C1). MioOcean BWT estimates decrease during the MMCT (14.7-13.8 Ma) and continue to decline until the end of the Miocene, reaching average values of 8.0°C using MioOcean calibration 1, 8.3°C using MioOcean calibration 2, and 6.9°C using the Lear et al., (2015). The latter is identical to the average BWT of 6.8°C originally reported by Lear et al. (2015) for the same interval. These differences in estimated

https://doi.org/10.5194/essd-2026-697
Preprint. Discussion started: 18 September 2026

BWT are due to the higher sensitivity (higher *H*-values) of our new equations to Mg/Ca_{sw}, which was reduced (<~3.0 mol/mol) during the MCO.

For the time interval 12.6 to 5.3 Ma at Site 806, our revised *C. wuellerstorfi* calibration yields average BWT of 5.9°C (Figure 6a), comparable to the mean BWT of 5.5°C originally reported by Lear et al. (2003), but colder than all our *O. umbonatus* BWT calibrations considering 68% confidence intervals (Figure 6a). Using the 68% confidence intervals, we identify a BWT cooling trend at this site between the MCO and the Late Miocene across all calibrations for *O. umbonatus* and *C. wuellerstorfi* calibrations. For *O. umbonatus*, MioOcean calibrations 1 and 2 yield narrower mean 68% confidence intervals (1.9°C-2.1°C) than that of Lear et al. (2015; 3.7°C), whereas for revised *C. wuellerstorfi* calibration presents a ~0.5°C mean 68% confidence interval (Figure 6a; Appendix C: Fig. C1). Therefore, we put forth MioOcean calibration 2 for *O. umbonatus* and the revised *C. wuellerstorfi* calibration as our preferred choices due to their narrow uncertainty envelopes and species-specific calibration datasets. Further, MioOcean calibration 2 retains the temperature sensitivity from Lear et al. (2002) based on core-top Mg/Ca data.

At Site 926, *O. umbonatus* and *C. wuellerstorfi* Mg/Ca records continuously span the interval 11.8 to 5.3 Ma, in addition to an Early Miocene segment spanning 23.6 to 22.8 Ma for *O. umbonatus* measurements (Figure 6b). The *O. umbonatus* MioOcean calibration 2 yields average BWT of 7.4°C (±1.5°C) between 11.8 and 8.0 Ma (warmer than the BWT of 5.7°C originally published by Lear et al. (2003)), followed by a cooling step to average BWT of 6.0°C (±1.7°C) between 8.0 and 5.3 Ma. A comparable trend, but with colder BWTs, results from our revised *C. wuellerstorfi* calibration, with average BWT of 5.8°C (±0.5°C) from 11.8 to 8.0 Ma (originally estimated as 5.1°C by Lear et al. (2003)), cooling to 4.3°C (±0.4°C) between 8.0 and 5.3 Ma (estimated as 3.5°C by Lear et al. (2003)). BWT estimates for *O. umbonatus* using the Lear et al. (2015) calibration are ~0.5°C colder than those estimated with MioOcean calibrations 1 and 2, with their 68% confidence envelopes overlap substantially (Fig. D1).

In addition to comparing our MioOcean temperature estimates with previously published values, we also compare MioOcean preferred benthic calibrations for both epifaunal and infaunal Mg/Ca records to revised benthic Mg/Ca calibrations from Nauter-Alves et al. (2025). These multivariate global core top calibrations explicitly account for thermal and non-thermal controls (e.g., saturation state). Application of *O. umbonatus* calibration with MioOcean input parameters (*H*-value, MioOcean Mg/Ca_{sw}; Table 1) results in similar BWT values, with overlapping 68% confidence intervals (Fig. D2). This suggests both calibration scenarios are applicable for Miocene temperature reconstructions. However, application of Nauter-Alves et al. (2025) calibration for epifaunal Mg/Ca values results in unrealistic temperature values (Fig. D2). This is attributed to the limited Mg/Ca-temperature sensitivity and significant Mg/Ca-carbonate saturation based on the global *C. wuellerstorfi* core top calibration. Given that seven out of the 22 Miocene benthic Mg/Ca records compiled in this effort derive from *C. wuellerstorfi* records and/or combined species *C. wuellerstorfi* and *C. mundulus*, we report medium confidence BWTs with the MioOcean epifaunal calibration. These estimates are coherent with *O. umbonatus*-derived BWTs, and provide the basis for further work, including comparison with forthcoming records of saturation state (B, Sr, Li) and/or records from carbon cycle models.

3.3.3 Global BWT trends according to water depth

The compiled infaunal and epifaunal BWT records depict a long-term cooling trend between the MCO and Late Miocene, with relative BWT changes that are consistent with their water depths (Figure 7). As expected, median BWTs are 2.0-3.0°C colder at sites located at water depths greater than 3000 m (Site 926 and U1338) throughout the Miocene. Exceptions are relatively cold BWTs between 17.0 and 12.0 Ma derived from epifaunal *C. wuellerstorfi* measurements at the shallower (~1600-1700 m water depth) Sites 747 and 757. These estimates may be biased by its high sensitivity of *C. wuellerstorfi* to changes in carbonate saturation (section 3.3.2).

Regardless of ocean basin, all compiled sites record an Early Miocene average BWT of 6.4°C between 23.0 and 17.0 Ma, warming during the Middle Miocene to an average of 9.4°C between 17.0

https://doi.org/10.5194/essd-2026-697
Preprint. Discussion started: 18 September 2026

and 12.0 Ma, and subsequent cooling to an average BWT of 7.2°C between 12.0 and 5.3 Ma (Figure 7). Warm Middle Miocene BWTs could be biased by the fact that most estimates derive from shallower sites, which were not affected by widespread carbonate dissolution (e.g., Pälike et al., 2012). Substantive (2.0-3.0°C) Late Miocene BWT cooling, between 9.0 and 7.0 Ma, was detected across shallow and deep sites in our compilation.

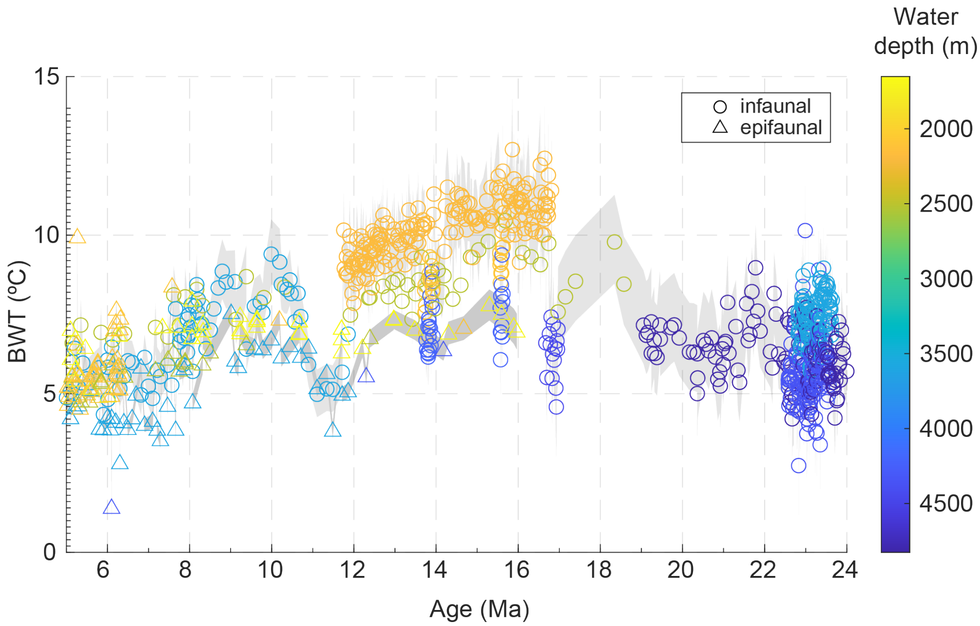

Figure 7. BWT estimates based on *O. umbonatus* (infaunal MioOcean calibration 2) and *C. wuellerstorfi* (epifaunal; updated Lo Giudice Cappelli et al. (2015) calibration). Contains all sites with benthic foraminifera compiled in the MioOcean initiative. Circles indicate infaunal and triangles indicate epifaunal benthics. Colour indicates modern water depth. Grey envelopes represent 68% confidence levels; dark-grey for epifaunal and light grey for infaunal BWTs.

3.4 Mg/Ca MioOcean temperature compilation

The MioOcean effort provides an ensemble-based UOT and BWT compilation for proxy and climate model users to easily use in future synthesis and proxy application efforts (Sosdian et al. this volume). We provide temperature estimates for multiple calibrations for both planktic and benthic Mg/Ca records, with robust uncertainty estimates that account for a variety of non-thermal variables that impact Mg/Ca observations. For Mg/Ca MioOcean UOT, we calculated temperatures using a Monte Carlo ensemble approach (N = 10,000 draws) using UOT scenarios from (1) both variants (pH-sensitive and pH-insensitive) of Gray & Evans, (2019) and (2) BAYMAG (Tierney et al 2019), assuming an Ω value of 5 (no dissolution correction). For the Mg/Ca MioOcean BWT we utilized "MioOcean 2" for infaunal scenarios (only *O. umbonatus*), based on narrower uncertainty envelopes and temperature sensitivity derived from Lear et al. (2002), and "bwt epifaunal cleancorr" for epifaunal scenarios (only *C. wuellerstorfi*).

4. Data availability

The MioMG data compilation is available as part of the MioOcean database (Sosdian et al., this volume) and is openly accessible and can be downloaded directly from the MioOcean website (https://www.miooocean.com/download-data/) or through Zenodo (https://doi.org/10.5281/zenodo.22258386, Sosdian et al. 2026). The record is currently restricted;

https://doi.org/10.5194/essd-2026-697
Preprint. Discussion started: 18 September 2026

editors and reviewers have access via a private link provided to the journal. Upon acceptance, the record will be made public under the same DOI. This includes newly compiled datasets for Mg/Ca-derived temperature and updated ages for Mg/Ca and Na/Ca datasets for key sites. We encourage users to also cite original data when using this data product, to provide credit to the data generators.

5. Code availability

All code used for the MioMG temperature compilation is publicly available on GitHub at https://github.com/audersea/mio_compilation. The record is currently restricted; editors and reviewers have access via a private link provided to the journal. Upon acceptance, the record will be made public under the same DOI. This includes code used for (1) compilation and extraction of MioMG Mg/Ca_{sw} curve for use in estimating temperature and (2) calculate temperatures from planktic and benthic Mg/Ca using various calibrations. The code for the Streamlit dashboard for MioMG is also on GitHub at https://github.com/audersea/mio_mg.

6. Conclusions and outlook

The MioOcean temperature compilation effort has provided the opportunity to review the existing framework for application of Mg/Ca paleothermometry in reconstructing temperatures across the Miocene. As part of this effort, the MioMG working group reviewed both planktic and benthic Mg/Ca calibrations and corresponding input parameters, Mg/Ca_{sw} constraints, present-day hydrographic conditions, and site-specific preservation. The result is a robust temperature compilation and Mg/Ca-paleothermometry framework that considers key uncertainties for estimating upper and deep ocean temperatures. Overall, the data coverage of UOT and BWT records across all ocean basins provides new insight into Miocene temperature trends and absolute temperatures during periods of sustained warmth. This synthesis will facilitate comparisons among multiple temperature proxies, analyses of spatial and temporal temperature trends, assessments of data-model mismatch, climate model validation, and ultimately a better understanding of the mechanisms driving Miocene climate change.

Most UOT Mg/Ca records are derived from the tropics, subtropics and some records from the Southern Ocean. Further, there is a fundamental lack of shallow water benthic Mg/Ca records from tropical and high latitude locations in the Northern Hemisphere that may be promising targets for future research. Orbitally resolved records are limited, and development of high-resolution cyclostratigraphy at selected sites would be useful as a springboard for evaluating the interplay between UOT and BWT and orbital-scale environmental variability.

For all foraminiferal Mg/Ca records, we used modern hydrographic conditions to help constrain the selection of available multivariable calibration scenarios when applying this paleothermometer to the Miocene, while considering likely site-specific changes in temperature, salinity, and pH. Additionally, best examples of preservation assessments used to document potential diagenetic alteration highlight that SEM and light microscopy images are useful to constrain key processes, but information is needed across stratigraphic layers to establish any changes with time, and a non-subjective reference for 'well-preserved' specimens is needed. Ideally, high resolution analysis of Miocene foraminifera would be used to examine retention of within-shell Mg/Ca banding akin to that observed in modern specimens. Further, we recommend that all future Mg/Ca publications provide, where available, a compilation of contamination data along with Mg/Ca to aid downcore assessment of diagenetic processes on a broader scale. We encourage authors to transparently and consistently report contamination data alongside of Mg/Ca measurements, together with the criteria used to exclude data. These criteria and approaches might be site-specific and include threshold values of multiple element-to-Ca ratios or elements (e.g., Fe, Al, Ti), correlation analysis between variables across time and within snapshot time intervals, identification of statistical outliers, and consideration of values that are outside of range for studied species.

Conversion of foraminiferal Mg/Ca to temperature requires archives of seawater Mg and Ca chemistry, and here we present a compilation that includes multiple proxy archives with corresponding

https://doi.org/10.5194/essd-2026-697
Preprint. Discussion started: 18 September 2026

uncertainty. Uncertainty in the Middle Miocene ocean temperatures are significant and divergent trends in proxy reconstructions limit the ability to reduce the uncertainty in temperature estimates during the MCO. Further work developing archives of shifts in $[Mg]_{sw}$ and $[Ca]_{sw}$ in the past are needed to reduce uncertainty in middle Miocene temperature estimates, critical for examining periods of global warmth.

Here we present Mg/Ca-derived UOT from a range of extant and extinct species from locations across the global oceans. To convert Mg/Ca to UOT we used multi-variable calibrations that include non-thermal factors (salinity, pH) and their Mg/Ca-sensitivity. One hurdle to reconstructing high confidence UOT is the effect of pH on Mg/Ca in some species, as we lack site-specific pH records. Across the Miocene, there are significant shifts in the oceanic carbonate system, with the lowest pH values during the MCO (Sosdian et al. 2018; Honisch et al. 2023). When employing pH-sensitive species, measuring corresponding pH records would be needed to best constrain UOT estimates. Further, more studies are needed to accurately determine the pH sensitivity of Mg/Ca for a range of different species under variable conditions of temperature, salinity, and growth rate, as these studies are rare due to the complexities of culturing planktic foraminifera. Additionally, lack of knowledge of pH sensitivity in extinct species increases uncertainty for corresponding UOT estimates. Future work is needed to assess the role of non-thermal factors on Miocene Mg/Ca variations in extinct species.

Our Mg/Ca proxy review also includes benthic Mg/Ca paleothermometry, and we refined existing calibrations for both infaunal and epifaunal foraminifera. In addition to Mg/Ca_{sw} uncertainty, less work has been done on the sensitivity of Mg/Ca_{foram} to Mg/Ca_{sw}, with a range of *H* values proposed for benthic foraminifera. We assess a range of scenarios and show that epifaunal and infaunal temperature reconstructions align across a range of *H* values and temperature sensitivity. To better quantify the uncertainty of Miocene BWT estimates, further constraints on the sensitivity of Mg/Ca_{foram} to Mg/Ca_{sw} is needed, as well as site-specific carbonate chemistry histories.

https://doi.org/10.5194/essd-2026-697
Preprint. Discussion started: 18 September 2026

7.0 Appendix

Appendix A: Foraminiferal Preservation Assessment

Figure A1 provides visual examples and supporting information for the assessment of foraminiferal preservation used in this study including planktic and benthic specimens spanning excellent to poor preservation.

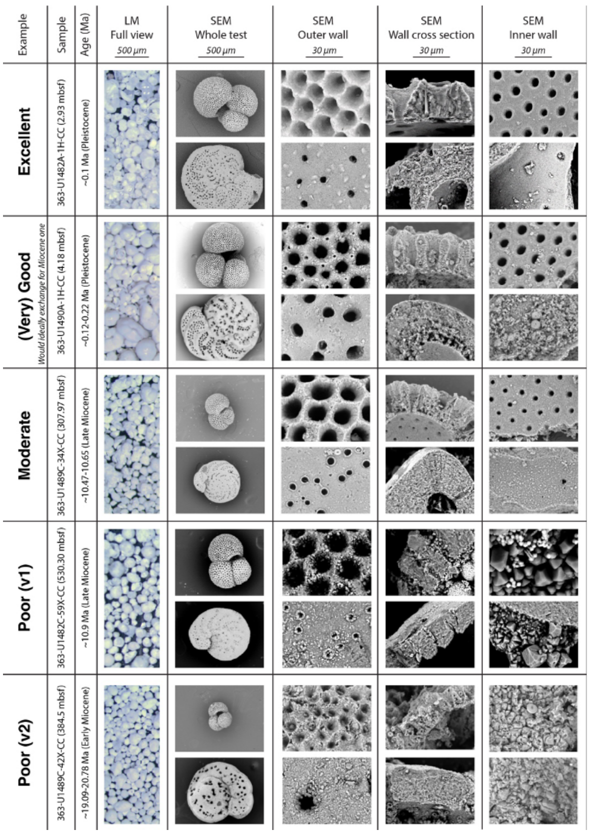

Figure A1: Examples of the multi-sample, multi-scale approach to visually assessing downcore foraminiferal preservation state developed during International ODP Expedition 363. Examples are shown of excellent, (very) good, moderate, and poor preservation for both planktic and benthic specimens. This figure is adapted from several figures in Rosenthal et al. (2018).

https://doi.org/10.5194/essd-2026-697
Preprint. Discussion started: 18 September 2026

Appendix B: MioOcean Mg/Ca$_{sw}$ compilation

Table B1 summarises the uncertainty range of the Mg/Ca$_{sw}$ curve generated in MioOcean, reporting the 2.5th, 16th, 50th, 84th, and 97.5th percentiles from a compilation of multiple proxy records. Figure B1 compares the resulting reconstruction from this study with previous proxy-derived and modelling-based Mg/Ca$_{sw}$ reconstructions, providing context for the compilation and its relationship to the reconstruction presented in Figure 3.

Table B1: 2.5th, 16th, 50th, 84th, and 97.5th percentiles of the Mg/Ca$_{sw}$ curve generated in MioOcean from compilation of range of proxies including halite fluid inclusions, CCVs, LBF, echinoderm ossicles, and Na/Ca records

	MioOcean Mg/Ca$_{sw}$ (mmol/mol)				
Age (Ma)	P05	P16	P50	P84	P95
0	4.98	5.08	5.21	5.37	5.47
1	4.82	4.95	5.14	5.34	5.48
2	4.61	4.73	4.96	5.17	5.30
3	4.31	4.44	4.65	4.84	5.00
4	3.99	4.11	4.29	4.47	4.58
5	3.67	3.79	3.95	4.12	4.21
6	3.41	3.51	3.70	3.86	3.98
7	3.20	3.33	3.52	3.70	3.83
8	3.06	3.20	3.40	3.60	3.74
9	2.98	3.11	3.31	3.52	3.67
10	2.92	3.07	3.27	3.46	3.60
11	2.92	3.05	3.23	3.40	3.53
12	2.88	2.98	3.15	3.31	3.41
13	2.76	2.87	3.03	3.19	3.27
14	2.60	2.74	2.91	3.09	3.21
15	2.37	2.56	2.82	3.06	3.24
16	2.17	2.37	2.75	3.09	3.34
17	2.05	2.32	2.78	3.18	3.49
18	2.08	2.34	2.84	3.31	3.62
19	2.15	2.41	2.90	3.41	3.68
20	2.16	2.50	3.00	3.45	3.77
21	2.19	2.52	3.01	3.50	3.79
22	2.29	2.57	3.02	3.46	3.77
23	2.37	2.62	3.01	3.44	3.67

https://doi.org/10.5194/essd-2026-697
Preprint. Discussion started: 18 September 2026

Open Access Earth System Science Data Discussions

24	2.30	2.57	2.99	3.37	3.62
25	2.18	2.44	2.86	3.25	3.56
26	1.98	2.27	2.64	3.09	3.40
27	1.90	2.14	2.45	2.84	3.13
28	1.93	2.08	2.28	2.55	2.80
29	1.93	2.03	2.16	2.35	2.49
30	1.92	2.01	2.11	2.24	2.35
31	1.93	2.00	2.10	2.20	2.29
32	1.95	2.01	2.13	2.27	2.35
33	1.93	2.04	2.20	2.42	2.59
34	1.87	2.07	2.31	2.66	2.96

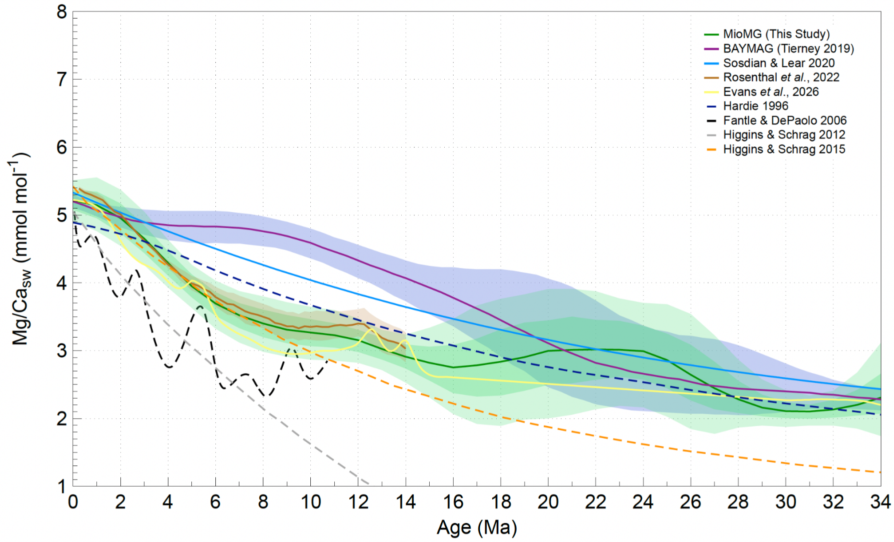

Figure B1: Mg/Ca_{sw} reconstructions from this study (MioMG) and previous proxy-derived efforts (BAYMAG: Tierney et al 2019; Sosdian & Lear 2020; Rosenthal et al. 2022; Evans et al. 2026) and modelling approaches (Hardie, 1996; Fantle & DePaolo, 2006; Higgins & Schrag, 2012; Higgins & Schrag, 2015). For MioMG compilation refer to Figure 3 and Table B1.

https://doi.org/10.5194/essd-2026-697
Preprint. Discussion started: 18 September 2026

Appendix C: BWT calibration scenarios

Figure C1 compares BWT estimates from *O. umbonatus* using the MioOcean calibration 1 and the calibration of Lear et al. (2015) at Sites 806 and 926, with envelopes representing 68% confidence intervals. Figure C2 compares BWT estimates from *O. umbonatus* and *C. wuellerstorfi* using the MioOcean preferred calibrations and those of Nauter-Alves et al. (2025) at Site 806, highlighting the influence of calibration choice on reconstructed BWT.

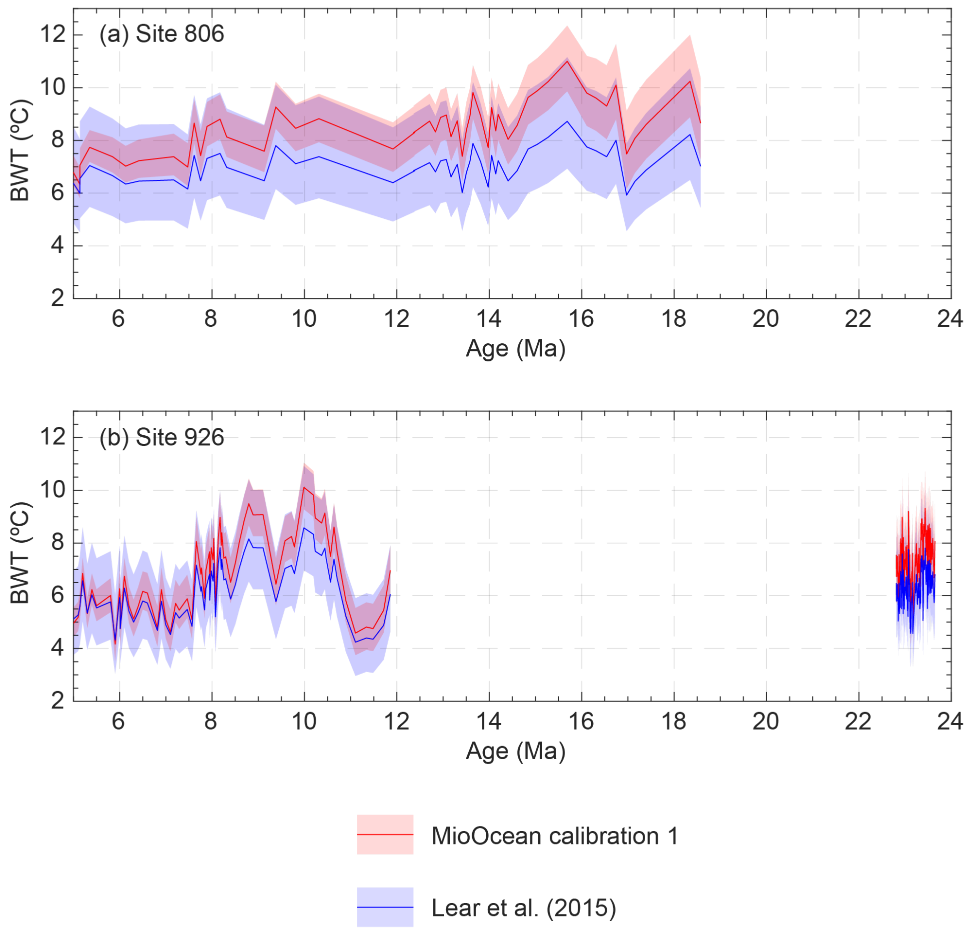

Figure C1: BWT estimates based on *O. umbonatus* Mg/Ca data using the MioOcean calibration 1 and that of Lear et al. (2015) for (a) Site 806 and (b) Site 926. Envelopes represent 68% confidence intervals.

https://doi.org/10.5194/essd-2026-697
Preprint. Discussion started: 18 September 2026

Open Access Earth System Science Data Discussions

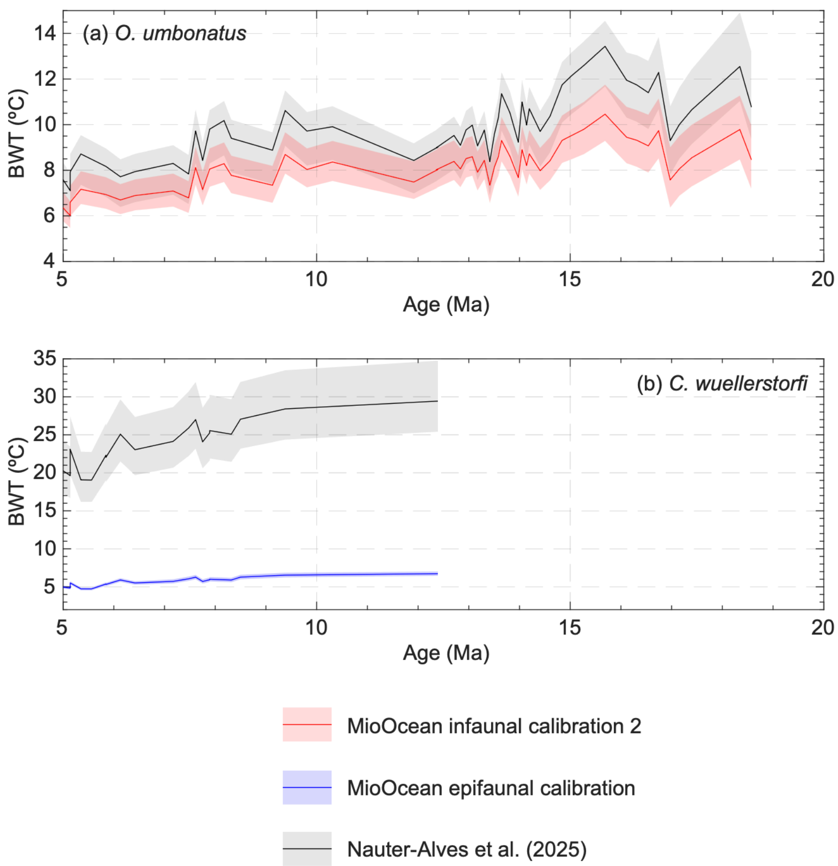

Figure C2: BWT estimates based on (a) *O. umbonatus* and (b) *C.* wuellerstorfi using MioOcean preferred calibration and those of Nauter-Alves et al. (2025) for Site 806. Envelopes represent 68% confidence intervals.

https://doi.org/10.5194/essd-2026-697
Preprint. Discussion started: 18 September 2026

8. Author contribution

MioMG: SS and KK contributed to conceptualization, data curation, formal analysis, investigation, methodology, project administration, supervision, validation, visualization, writing – original draft preparation, and writing – review and editing. AH contributed to conceptualization, data curation, formal analysis, investigation, methodology, project administration, supervision, validation, and visualization. CB contributed to conceptualization, data curation, investigation, methodology, validation, visualization, and writing – review and editing. AJD contributed to conceptualization, data curation, investigation, methodology, validation, visualization, writing – original draft preparation, and writing – review and editing. EJ contributed to conceptualization, data curation, formal analysis, investigation, methodology, code development, supervision, validation, visualization, writing – original draft preparation, and writing – review and editing. WK and CHL contributed to conceptualization, data curation, investigation, methodology, validation, visualization, and writing – review and editing. PM contributed to conceptualization, data curation, investigation, methodology, validation, visualization, writing – original draft preparation, and writing – review and editing. AA contributed to proxy code development, validation, and visualization.

MioOcean: SS, AA, SM, and AH contributed to MioOcean funding acquisition, MioOcean project administration, and MioOcean supervision.

9. Competing interests

The authors declare that they have no conflict of interest.

10. Acknowledgements

We acknowledge the financial support provided by the PAGES and UKIODP to hold MioOcean meetings and workshops. We also gratefully acknowledge the support of the PAGES Data Stewardship Scholarship (DSS) as part of the PlioMioVar working group, which contributed to the development of the MioOcean database, compilation pipeline, and visualization tools. We acknowledge the Miocene Temperature Data Portal (https://bolin.su.se/data/miocene-temperature-portal) as a starting point for this compilation, and the Gulf Coast, Bremen, and Kochi core repositories for IODP and related core samples and information which underpin the MioMG work. We thank Xiaoqing Liu for assistance with the production of Figure 2 and David Evans with support in BWT calculations using the "El/CaRBenthic" Matlab code and data analysis for Figure D2. We acknowledge wider financial funding as follows: CTB acknowledges the French National Research Agency (project ANR-22-EDIR-0003) for funding. CL acknowledges the Past to Future (P2F) project that has received funding from the European Union's Horizon Europe research and innovation programme under grant agreement No. 101184070 and K.G.D.K. is supported by ERC grant (HighBorG, 101125914): both funded by the European Union. For EU funded work, views and opinions expressed are however those of the author(s) only and do not necessarily reflect those of the European Union or the European Climate, Infrastructure and Environment Executive Agency (CINEA). Neither the European Union nor the granting authority can be held responsible for them. For the purpose of Open Access, the author(s) have applied a Creative Commons license to any Author Accepted Manuscript (AAM) version arising from this submission.

11. References

Agterhuis, T., Ziegler, M., de Winter, N. J., and Lourens, L. J.: Warm deep-sea temperatures across Eocene Thermal Maximum 2 from clumped isotope thermometry, Communications Earth & Environment, 3, 39, 10.1038/s43247-022-00350-8, 2022.

Anand, P., Elderfield, H., and Conte, M. H.: Calibration of Mg/Ca thermometry in planktonic foraminifera from a sediment trap time series, Paleoceanography, 18, 10.1029/2002PA000846, 2003.

Anderson, L. B., Hönisch, B., Coxall, H. K., and Bolge, L.: Atmospheric CO2 estimates for the late Oligocene and early Miocene using multi-species cross-calibrations of boron isotopes. Paleoceanography and Paleoclimatology, 39, e2022PA004569, https://doi.org/10.1029/2022PA004569, 2024.

Aze, T., Ezard, T. H. G., Purvis, A., Coxall, H. K., Stewart, D. R. M., Wade, B. S., and Pearson, P. N.: A phylogeny of Cenozoic macroperforate planktonic foraminifera from fossil data, Biological Reviews, 86, 900-927, https://doi.org/10.1111/j.1469-185X.2011.00178.x, 2011.

Badger, M. P. S., Lear, C. H., Pancost, R. D., Foster, G. L., Bailey, T. R., Leng, M. J., and Abels, H. A.: CO2 drawdown following the middle Miocene expansion of the Antarctic Ice Sheet, Paleoceanography, 28, 10.1002/palo.20015, 2013.

Barker, S., Greaves, M., and Elderfield, H.: A study of cleaning procedures used for foraminiferal Mg/Ca paleothermometry, Geochemistry Geophysics Geosystems, 4, 10.1029/2003gc000559, 2003.

BAYMAG: A Bayesian framework for reconstructing past seawater temperature and $\delta^{18}O$: https://github.com/jesstierney/BAYMAG, last access: August 20 2026.

Billups, K., and Scheiderich, K.: A synthesis of Late Oligocene through Miocene deep sea temperatures as inferred from foraminiferal Mg/Ca ratios. International Association of Sedimentology, Special Publication, 42, 1-16. doi:10.1002/9781118398364.ch1, 2012.

Billups, K., and Schrag, D. P.: Paleotemperatures and ice volume of the past 27 Myr revisited with paired Mg/Ca and 18O/16O measurements on benthic foraminifera. Paleoceanography, 17(1). DOI:10.1029/2000PA000567, 2002.

Billups, K. and Schrag, D.P.: Application of benthic foraminiferal Mg/Ca ratios to questions of Cenozoic climate change. Earth and Planetary Science Letters, 209(1-2), 181-195, https://doi.org/10.1016/S0012-821X(03)00067-0, 2003.

Boscolo-Galazzo, F., Crichton, K. A., Ridgwell, A., Mawbey, E. M., Wade, B. S., and Pearson, P. N.: Temperature controls carbon cycling and biological evolution in the ocean twilight zone, Science, 371, 1148-1152, 10.1126/science.abb6643, 2021.

Boscolo-Galazzo, F., Evans, D., Mawbey, E. M., Gray, W. R., Pearson, P. N., and Wade, B. S.: Exploring macroevolutionary links in multi-species planktonic foraminiferal Mg/Ca and $\delta^{18}O$ from 15 Ma to recent, Biogeosciences, 22, 1095-1113, 10.5194/bg-22-1095-2025, 2025.

Boyer, T. P., Antonov, J. I., Baranova, O. K., Garcia, H. E., Johnson, D. R., Mishonov, A. V., O'Brien, T. D., Seidov, D., Smolyar, I., Zweng, M. M., Paver, C. R., Locarnini, R. A., Reagan, J. R., Forgy, C., Grodsky, A., and Levitus, S.: World ocean database 2013, http://doi.org/10.7289/V5NZ85MT, 2013.

Brennan, S. T., Lowenstein, T. K., and Cendon, D. I.: The major-ion composition of Cenozoic seawater: The past 36 million years from fluid inclusions in marine halite, American Journal of Science, 313, 713-775, DOI: 10.2475/08.2013.01, 2013.

Broecker, W. S. and Peng, T.-H., Columbia University (Ed.): Tracers in the Sea, Lamont-Doherty Geological Observatory., New York, 1982.

Burkett, A. M.: Life on Plastics: Deep-Sea Foraminiferal Colonization Patterns and Reproductive Morphology, Journal of Marine Science and Engineering, 13, 1597, 10.3390/jmse13081597, 2025.

Burls, N. J., Bradshaw, C. D., De Boer, A. M., Herold, N., Huber, M., Pound, M., Donnadieu, Y., Farnsworth, A., Frigola, A., Gasson, E., von der Heydt, A. S., Hutchinson, D. K., Knorr, G., Lawrence, K. T., Lear, C. H., Li, X., Lohmann, G., Lunt, D. J., Marzocchi, A., Prange, M., Riihimaki,

https://doi.org/10.5194/essd-2026-697
Preprint. Discussion started: 18 September 2026

Open Access Earth System Science Data Discussions

C. A., Sarr, A.-C., Siler, N., and Zhang, Z.: Simulating Miocene warmth: Insights from an opportunistic multi-model ensemble (MioMIP1)Paleoceanography and Paleoclimatology, 36, e2020PA004054. https://doi.org/10.1029/2020PA004054, 2021.

Chaabane, S., Schiebel, R., Meilland, J., Brummer, G. J. A., Mortyn, P. G., Sulpis, O., Chalk, T. B., Giraud, X., Howa, H., Kuroyanagi, A., Beaugrand, G., and de Garidel-Thoron, T.: Reassessment of the global distribution and diversity of modern planktonic foraminifera from the FORCIS database, J. Micropalaeontol., 45, 195-217, 10.5194/jm-45-195-2026, 2026.

Chave, K.E.: Aspects of the Biogeochemistry of Magnesium 1. Calcareous Marine Organisms. The Journal of Geology, 62 (3), 266-283. DOI: 10.1086/626162, 1954.

Clarke, F.W. and Wheeler, W.C.: The inorganic constituents of marine invertebrates. USGS Professional Paper 124, 62 pp. DOI: 10.3133/pp124, 1922.

Chilingar, G.V.: Dependance on temperature of Ca/Mg ratio of skeletal structures of organisms and direct chemical precipitates out of seawater. Bulletin of the Southern Californian Academie of Sciences 61, 45-60. DOI: 10.3160/0038-3872-61.1.45, 1962.

Coggon, R. M., Teagle, D. A., Smith-Duque, C. E., Alt, J. C., and Cooper, M. J.: Reconstructing past seawater Mg/Ca and Sr/Ca from mid-ocean ridge flank calcium carbonate veins. Science, 327 (5969), 1114–1117, DOI: 10.1126/science.1182252, 2010.

Cramer, B. S., Toggweiler, J. R., Wright, J. D., Katz, M. E., and Miller, K. G.: Ocean overturning since the Late Cretaceous: Inferences from a new benthic foraminiferal isotope compilation, Paleoceanography, 24, PA4216, doi:10.1029/2008PA001683, 2009.

Dekens, P. S., Lea, D. W., Pak, D. K., and Spero, H. J.: Core top calibration of Mg/Ca in tropical foraminifera: Refining paleotemperature estimation, Geochemistry, Geophysics, Geosystems, 3, 1-29, https://doi.org/10.1029/2001GC000200, 2002.

Delaney, M. L., Be, A. W. H., and Boyle, E. A.: Li, Sr, Mg, and Na in foraminiferal calcite shells from laboratory culture, sediment traps, and sediment cores, *Geochimica et Cosmochimica Acta*, 49, 1327–1341, https://doi.org/10.1016/0016-7037(85)90284-4, 1985.

Detlef, H., Sosdian, S. M., Kender, S., Lear, C. H., and Hall, I. R.: Multi-elemental composition of authigenic carbonates in benthic foraminifera from the eastern Bering Sea continental margin (International Ocean Discovery Program Site U1343), Geochimica et Cosmochimica Acta, 268, 1-21, https://doi.org/10.1016/j.gca.2019.09.025, 2020.

Dickson, J.: Fossil Echinoderms as Monitor of the Mg/Ca Ratio of Phanerozoic Oceans. Science 298 (5596),1222-1224, DOI: 10.1126/science.1075882, 2002

Dickson, J.: Echinoderm Skeletal Preservation: Calcite-Aragonite Seas and the Mg/Ca Ratio of Phanerozoic Oceans. Journal of Sedimentary Research. 74. 355-365, DOI: 10.1306/112203740355, 2004.

Drury et al., this volume refers to ESSD companion paper with the following manuscript information: Anna Joy Drury, Deborah N. Tangunan, Gerald Auer, Jennifer Kasbohm, David J. King, Anya J. Crocker, Karlos G. D. Kochhann, Wolfgang Kuhnt, Diana Ochoa, Marci M. Robinson, Thomas Westerhold, Tim E. van Peer, Diederik Liebrand, Wout Krijgsman, Bridget S. Wade, Elizabeth C. Sibert, Neeraj S. Shah, Sindia M. Sosdian, Sevasti Modestou, Alexandra Auderset, and Ann Holbourn.: The MioOcean Age Framework: An Age Model Database and Chronoinformatics Approach for synchronised Miocene Ocean Temperature, Climate and Proxy Records. ESSD Manuscript Reference essd-2026-724.

Drury, A. J., Lee, G. P., Pennock, G. M., and John, C. M.: Data report: Late Miocene to early Pliocene coccolithophore and foraminiferal preservation at Site U1338 from scanning

https://doi.org/10.5194/essd-2026-697
Preprint. Discussion started: 18 September 2026

electron microscopy, in: *Proceedings of the Integrated Ocean Drilling Program*, edited by Pälike, H., et al., Integrated Ocean Drilling Program Management International, Inc., Tokyo, 2014.

Drury, A. J., Lee, G. P., Gray, W. R., Lyle, M., Westerhold, T., Shevenell, A. E., and John, C. M.: Deciphering the State of the Late Miocene to Early Pliocene Equatorial Pacific, Paleoceanography and Paleoclimatology, 33, 246-263, https://doi.org/10.1002/2017PA003245, 2018.

Dueñas-Bohórquez, A., da Rocha, R.E., Kuroyanagi, A., Bijma, J., and Reichart, G.-J.: Effect of salinity and seawater calcite saturation state on Mg and Sr incorporation in cultured planktonic foraminifera, Marine Micropaleontology, 73, 178 189, doi:10.1016/j.marmicro.2009.09.002, 2009.

Edgar, K. M., Pälike, H., and Wilson, P. A.: Testing the impact of diagenesis on the $\delta^{18}O$ and $\delta^{13}C$ of benthic foraminiferal calcite from a sediment burial depth transect in the equatorial Pacific, Paleoceanography, 28, 468-480, https://doi.org/10.1002/palo.20045, 2013.

Edgar, K. M., Anagnostou, E., Pearson, P. N., and Foster, G. L.: Assessing the impact of diagenesis on $\delta^{11}B$, $\delta^{13}C$, $\delta^{18}O$, Sr/Ca and B/Ca values in fossil planktic foraminiferal calcite, Geochimica et Cosmochimica Acta, 166, 189-209, https://doi.org/10.1016/j.gca.2015.06.018, 2015.

Elderfield, H., and Ganssen, G.: Past temperature and $\delta^{18}O$ of surface ocean waters inferred from foraminiferal Mg/Ca ratios. Nature 405, 442–445 (2000). https://doi.org/10.1038/35013033, 2000.

Elderfield, H., Vautravers, M., and Cooper, M.: The relationship between shell size and Mg/Ca, Sr/Ca, $\delta^{18}O$, and $\delta^{13}C$ of species of planktonic foraminifera, Geochemistry, Geophysics, Geosystems, 3, 1-13, https://doi.org/10.1029/2001GC000194, 2002

Elderfield, H., Yu, J., Anand, P., Kiefer, T., and Nyland, B.: Calibrations for benthic foraminiferal Mg/Ca paleothermometry and the carbonate ion hypothesis. Earth and Planetary Science Letters, 250, 633–649, doi:10.1016/j.epsl.2006.07.041, 2006.

Evans, D., Erez, J., Oron, S., and Müller, W.: Mg/Ca-temperature and seawater-test chemistry relationships in the shallow-dwelling large benthic foraminifera Operculina ammonoides, Geochimica et Cosmochimica Acta, 148, 325-342, https://doi.org/10.1016/j.gca.2014.09.039, 2015.

Evans, D., Brierley, C., Raymo, M. E., Erez, J., and Müller, W.: Planktic foraminifera shell chemistry response to seawater chemistry: Pliocene–Pleistocene seawater Mg/Ca, temperature and sea level change, Earth and Planetary Science Letters, 438, 139-148, https://doi.org/10.1016/j.epsl.2016.01.013, 2016.

Evans, D., Sagoo, N., Renema, W., Cotton, L. J., Müller, W., Todd, J. A., Saraswati, P.K., Stassen, P., Ziegler, M., Pearson, P.N., Valdes, P.J., and Affek, H. P.: Eocene greenhouse climate revealed by coupled clumped isotope-Mg/Ca thermometry. Proc. Natl. Acad. Sci. U.S.A. 115 (6) , 1174–1179, https://doi.org/10.1073/pnas.1714744115, 2018.

Evans, D., Rosenthal, Y., Erez, J., Hauzer, H., Cotton, L., Zhou, X., Nambiar, R., Stassen, P., Pearson, P.N., Renema, W., Saraswati, P.K., Todd, J.A., Müller, W., and Affek, H.P.: The major ion chemistry of seawater was closely coupled to the long-term carbon cycle during the Cenozoic. PNAS 123 (2) e2511781122. https://doi.org/10.1073/pnas.2511781122, 2026.

Fantle, M.S., and DePaolo, D.J.: Sr isotopes and pore fluid chemistry in carbonate sediment of the Ontong Java Plateau: calcite recrystallization rates and evidence for a rapid rise in seawater Mg over the last 10 million years. Geochimica et Cosmochimica Acta, 70, 3883–3904, 2006.

Foster, G. L., Lear, C. H., Rae, J. W. B.: The evolution of pCO_2, ice volume and climate during the middle Miocene. Earth and Planetary Science Letters, 341-344, 243-254, https://doi.org/10.1016/j.epsl.2012.06.007, 2012.

https://doi.org/10.5194/essd-2026-697
Preprint. Discussion started: 18 September 2026

Fox, L. R. and Wade, B. S.: Systematic taxobomy of early-middle Miocene planktonic foraminifera from the equatorial Pacific Ocean: Integrated Ocean Drilling Program, Site U1338, Journal of Foraminiferal Research, 43, 374-405, DOI: 10.2113/gsjfr.43.4.374, 2013.

Fox, L. R.: Mid Miocene orbital climate variability and biotic response in the Pacific Ocean, PhD thesis, School of Earth and Environment, University of Leeds, 2014

Fox, L. R., Wade, B. S., Holbourn, A., Leng, M. J., and Bhatia, R.: Temperature Gradients Across the Pacific Ocean During the Middle Miocene, Paleoceanography and Paleoclimatology, 36, e2020PA003924, https://doi.org/10.1029/2020PA003924, 2021.
Friedrich, O., Schiebel, R., Wilson, P. A., Weldeab, S., Beer, C. J., Cooper, M. J., and Fiebig, J.: Influence of test size, water depth, and ecology on Mg/Ca, Sr/Ca, δ18O and δ13C in nine modern species of planktic foraminifers, Earth and Planetary Science Letters, 319-320, 133-145, https://doi.org/10.1016/j.epsl.2011.12.002, 2012.

Fukuda, K., Thomas, D. B., Frew, R. D., and Ewan Fordyce, R.: Antarctic glaciation recorded in Early Miocene New Zealand foraminifera. Marine Micropaleontology, 92-93. DOI:10.1016/j.marmicro.2012.05.002, 2012.

Gothmann, A. M., Stolarski, J., Adkins, J. F., Schoene, B., Dennis, K. J., Schrag, D. P., Mazur, M., and Bender, M. L.: Fossil corals as an archive of secular variations in seawater chemistry since the Mesozoic, Geochimica et Cosmochimica Acta, 160, 188–208, DOI: 10.1016/j.gca.2015.03.018, 2015.

Gray, W. R., and Evans, D.: Nonthermal influences on Mg/Ca in planktonic foraminifera: A review of culture studies and application to the last glacial maximum. Paleoceanography and Paleoclimatology, 34, 306–315. https://doi.org/10.1029/2018PA003517, 2019.

Greenop, R., Sosdian, S. M., Henehan, M. J., Wilson, P. A., Lear, C. H., and Foster, G. L.: Orbital Forcing, Ice Volume, and CO2 Across the Oligocene-Miocene Transition, Paleoceanography and Paleoclimatology, 34, 316-328, https://doi.org/10.1029/2018PA003420, 2019.

Guillermic, M., Misra, S., Eagle, R., and Tripati, A.: Atmospheric CO_2 estimates for the Miocene to Pleistocene based on foraminiferal $\delta^{11}B$ at Ocean Drilling Program Sites 806 and 807 in the Western Equatorial Pacific, Clim. Past, 18, 183–207, https://doi.org/10.5194/cp-18-183-2022, 2022.

Hardy, L.A.: Secular variation in seawater chemistry: An explanation for the coupled secular variation in the mineralogies of marine limestones and potash evaporites over the past 600 m.y. Geology 24 (3), 279–283, https://doi.org/10.1130/0091-7613(1996)024<0279:SVISCA>2.3.CO;2, 1996

Hasenfratz, A. P., Schiebel, R., Thornalley, D. J. R., Schönfeld, J., Jaccard, S. L., Martínez-García, A., Holbourn, A., Jennings, A. E., Kuhnt, W., Lear, C. H., Marchitto, T. M., Quillmann, U., Rosenthal, Y., Yu, J., and Haug, G. H.: Mg/Ca-temperature calibration for the benthic foraminifera Melonis barleeanum and Melonis pompilioides, Geochimica et Cosmochimica Acta, 217, 365-383, https://doi.org/10.1016/j.gca.2017.08.038, 2017.
Hasiuk, F. J. and Lohmann, K. C.: Application of calcite Mg partitioning functions to the reconstruction of paleocean Mg/Ca, Geochimica Et Cosmochimica Acta, 74, 6751-6763, 10.1016/j.gca.2010.07.030, 2010.

Healey, S. L., Thunell, R. C. and Corliss, B. H.: The Mg/Ca-temperature relationship of benthic foraminiferal calcite: New core-top calibrations in the <4 °C temperature range. Earth and Planetary Science Letters, 272, 523–530, doi:10.1016/j.epsl.2008.05.023, 2008.

Hess, A. V., Auderset, A., Rosenthal, Y., Miller, K. G., Zhou, X., Sigman, D. M., and Martínez-García, A.: A well-oxygenated eastern tropical Pacific during the warm Miocene, Nature, 619, 521-525, 10.1038/s41586-023-06104-6, 2023.

Higgins, J. A., and Schrag, D. P.: Records of Neogene seawater chemistry and diagenesis in deep-sea carbonate sediments and pore fluids. Earth Planet. Sci. Lett. 357-358, 386-396, http://dx.doi.org/10.1016/j.epsl.2012.08.030, 2012.

Higgins, J. A., and Schrag, D. P.: The Mg isotopic composition of Cenozoic seawater–Evidence for a link between Mg-clays, seawater Mg/Ca, and climate. Earth Planet. Sci. Lett. 416, 73–81, http://dx.doi.org/10.1016/j.epsl.2015.01.003, 2015.

Hilgen, F. J., Lourens, L. J., and Van Dam, J. A.: The Neogene Period. In Gradstein, F. M., Ogg, J. G., Schmitz, M. D., and Ogg, G. M. (editors), The Geologic Timescale 2012, Elsevier Publisher, 923-978, DOI: 10.1016/B978-0-444-59425-9.00029-9, 2012

Holbourn, A., Kuhnt, W., Regenberg, M., Schulz, M., Mix, A. C., and Andersen, N.: Does Antarctic glaciation force migration of the tropical rain belt? Geology, 38(9), 783-786. DOI:10.1130/G31043.1, 2010.

Holbourn, A. E., Henderson, A. S., and MacLeod, N.: Atlas of Benthic Foraminifera, Wiley-Blackwell, Chichester, UK, 2013.

Holbourn, A., Kuhnt, W., Clemens, S. C., Kochhann, K. G. D., Jöhnck, J., Lübbers, J., and Andersen, N.: Late Miocene climate cooling and intensification of southeast Asian winter monsoon. Nature Communications, 9(1). DOI:10.1038/s41467-018-03950-1, 2018.

Holbourn, A., Kuhnt, W., Clemens, S. C., and Heslop, D.: A ~12 Myr Miocene Record of East Asian Monsoon Variability From the South China Sea, Paleoceanography and Paleoclimatology, 36, e2021PA004267, https://doi.org/10.1029/2021PA004267, 2021.

Hönisch, B., Allen, K. A., Lea, D. W., Spero, H. J., Eggins, S. M., Arbuszewski, J., deMenocal, P., Rosenthal, J., Russell, A.D., and Elderfield, H.: The influence of salinity on Mg/Ca in planktic foraminifers – Evidence from cultures, core-top sediments and complementary $\delta^{18}O$. Geochimica et Cosmochimica Acta, 121, 196–213, http://dx.doi.org/10.1016/j.gca.2013.07.028, 2013.

Holland, K., Branson, O., Haynes, L. L., Hönisch, B., Allen, K. A., Russell, A. D., and Eggins, S. M.: Constraining multiple controls on planktic foraminifera Mg/Ca. Geochimica et Cosmochimica Acta, 273, 116–136. https://doi.org/10.1016/j.gca.2020.01.015, 2020.

Horita, J., Zimmermann, H., and Holland, H. D.: Chemical evolution of seawater during the Phanerozoic: Implications from the record of marine evaporites, Geochimica Et Cosmochimica Acta, 66, 3733-3756, 10.1016/s0016-7037(01)00884-5, 2002.

John, E. H., Staudigel, P. T., Buse, B., Lear, C. H., Pearson, P. N., and Slater, S. M.: Revealing Their True Stripes: Mg/Ca Banding in the Paleogene Planktonic Foraminifera Genus Morozovella and Implications for Paleothermometry, Paleoceanography and Paleoclimatology, 38, e2023PA004652, https://doi.org/10.1029/2023PA004652, 2023.

Jöhnck, J., Kuhnt, W., Holbourn, A., and Andersen, N.: Variability of the Indian Monsoon in the Andaman Sea across the Miocene-Pliocene transition. Paleoceanography and Paleoclimatology, 35, e2020PA003923. doi:10.1029/2020PA003923, 2020.

Johnstone, H. J. H., Steinke, S., Kuhnert, H., Bickert, T., Pälike, H., and Mohtadi, M.: Automated cleaning of foraminifera shells before Mg/Ca analysis using a pipette robot, Geochemistry, Geophysics, Geosystems, 17, 3502-3511, https://doi.org/10.1002/2016GC006422, 2016.

Jones, R. W.: The Challenger Foraminifera, Oxford University Press, New York, 1994.

Kennett, J. P. and Srinivasan, M. S.: Neogene Planktonic Foraminifera: A Phylogenetic Atlas, Hutchinson and Ross, Stroudsburg,1983.

Kısakürek, B., Eisenhauer. A., Böhm, F., Garbe-Schönberg, D., Erez, J.: Controls on shell Mg/Ca and Sr/Ca in cultured planktonic foraminiferan, Globigerinoides ruber (white). Earth and Planetary Science Letters, 273, 260–269, doi:10.1016/j.epsl.2008.06.026, 2008.

Kochhann, K. G. D., Holbourn, A., Kuhnt, W., Channell, J. E. T., Lyle, M., Shackford, J. K., Wilkens, R. H., and Andersen, N.: Eccentricity pacing of eastern equatorial Pacific carbonate dissolution cycles during the Miocene Climatic Optimum, Paleoceanography, 31, 1176-1192, https://doi.org/10.1002/2016PA002988, 2016.

Kochhann, K. G. D., Holbourn, A., Kuhnt, W., and Xu, J.: Eastern equatorial Pacific benthic foraminiferal distribution and deep water temperature changes during the early to middle Miocene, Marine Micropaleontology, 133, 28-39, https://doi.org/10.1016/j.marmicro.2017.05.002, 2017.

Kubota, Y., Kimoto, K., Itaki, T., Yokoyama, Y., Miyairi, Y., and Matsuzaki, H.: Bottom water variability in the subtropical northwestern Pacific from 26 kyr BP to present based on Mg / Ca and stable carbon and oxygen isotopes of benthic foraminifera, Clim. Past, 11, 803-824, 10.5194/cp-11-803-2015, 2015.

Kuhnert, H., Bickert, T., and Paulsen, H.: Southern Ocean frontal system changes precede Antarctic ice sheet growth during the middle Miocene, Earth and Planetary Science Letters, 284, 630-638, https://doi.org/10.1016/j.epsl.2009.05.030, 2009.

Lauvset, S. K., Key, R. M., Olsen, A., van Heuven, S., Velo, A., Lin, X., Schirnick, C., Kozyr, A., Tanhua, T., Hoppema, M. Jutterström, S., Steinfeldt, R., Jeansson, E., Ishii, M., Perez, F. F., Suzuki, T., and Watelet, S. (2016). A new global interior ocean mapped climatology: the 1° × 1° GLODAP version 2. Earth Syst. Sci. Data, 8(2), 325–340. http://doi.org/10.5194/essd-8-325-2016, 2016

Lamyman, G. S., Fordham, B. G., Pearson, P. N., Wade, B. S., Woodhouse, A., Young, J. R., and Aze, T.: Phylogeny of the Cenozoic planktonic foraminifera, Journal of Systematic Palaeontology, 24, 2669255, 10.1080/14772019.2026.2669255, 2026.

Lawrence, K., Coxall, H., Sosdian, S., and Steinthorsdottir, M.: Miocene temperature portal. Dataset version 1. Bolin Centre Database. https://doi.org/10.17043/miocene-temperature-portal-1, 2021

Lea, D. W., Mashiotta, T. A., and Spero, H.J.: Controls on magnesium and strontium uptake in planktonic foraminifera determined by live culturing. Geochimica et Cosmochimica Acta, 63, 16, 2369–2379,

Lear, C. H., Coxall, H. K. Foster, G. L., Lunt, D. J., Mawbey, E. M., Rosenthal, Y., Sosdian, S. M., Thomas, E., and Wilson P. A.: Neogene ice volume and ocean temperatures: Insights from infaunal foraminiferal Mg/Ca paleothermometry, Paleoceanography, 30, 1437–1454, doi:10.1002/2015PA002833, 2015.

Lear, C. H., Elderfield, H., and Wilson, P. A.: Cenozoic deep-sea temperatures and global ice volumes from Mg/Ca in benthic foraminiferal calcite, Science, 287, 269-272, 10.1126/science.287.5451.269, 2000.

Lear, C. H., Mawbey, E. M., and Rosenthal, Y.: Cenozoic benthic foraminiferal Mg/Ca and Li/Ca records: Toward unlocking temperatures and saturation states, Paleoceanography, 25, https://doi.org/10.1029/2009PA001880, 2010.

Lear, C. H., Rosenthal, Y., and Slowey, N.: Benthic foraminiferal Mg/Ca-paleothermometry: A revised core-top calibration, Geochimica Et Cosmochimica Acta, 66, 3375-3387, 10.1016/s0016-7037(02)00941-9, 2002.

Lear, C. H., Rosenthal, Y., and Wright, J.D.: The closing of a seaway: ocean water masses and global climate change. Earth and Planetary Science Letters, 210, 425-436, DOI:10.1016/S0012-821X(03)00164-X, 2003.

https://doi.org/10.5194/essd-2026-697
Preprint. Discussion started: 18 September 2026

Lebrato, M., Garbe-Schönberg, D., Müller, M. N., Blanco-Ameijeiras, S., Feely, R. A., Lorenzoni, L., Molinero, J.-C., Bremer, K., Jones, D. O. B., Iglesias-Rodriguez, D., Greeley, D., Lamare, M. D., Paulmier, A., Graco, M., Cartes, J., Barcelos e Ramos, J., de Lara, A., Sanchez-Leal, R., Jimenez, P., Paparazzo, F. E., Hartman, S. E., Westernströer, U., Küter, M., Benavides, R., da Silva, A. F., Bell, S., Payne, C., Olafsdottir, S., Robinson, K., Jantunen, L. M., Korablev, A., Webster, R. J., Jones, E. M., Gilg, O., Bailly du Bois, P., Beldowski, J., Ashjian, C., Yahia, N. D., Twining, B., Chen, X.-G., Tseng, L.-C., Hwang, J.-S., Dahms, H.-U., and Oschlies, A.: Global variability in seawater Mg:Ca and Sr:Ca ratios in the modern ocean, Proceedings of the National Academy of Sciences, 117, 22281-22292, 10.1073/pnas.1918943117, 2020.

Liu, X., Huber, M., Foster, G.L., Dessler, A., and Zhang, Y.G.: Persistent high latitude amplification of the Pacific Ocean over the past 10 million years. Nature Communications 13, 7310, https://doi.org/10.1038/s41467-022-35011-z, 2022.

Lübbers, J., Kuhnt, W., Holbourn, A. E., Bolton, C. T., Gray, E., Usui, Y., Kochhann, K. G. D., Beil, S., and Andersen, N.: The Middle to Late Miocene "Carbonate Crash" in the Equatorial Indian Ocean, Paleoceanography and Paleoclimatology, 34, 813-832, https://doi.org/10.1029/2018PA003482, 2019.

Martin, P. A. and Lea, D. W.: A simple evaluation of cleaning procedures on fossil benthic foraminiferal Mg/Ca, Geochemistry, Geophysics, Geosystems, 3, 1-8, https://doi.org/10.1029/2001GC000280, 2002.

Martin, P. A., Lea, D.W., Rosenthal, Y., Shackleton, N. J., Sarnthein, M., Papenfuss, T.: Quaternary deep sea temperature histories derived from benthic foraminiferal Mg/Ca, Earth and Planetary Science Letters, 198, 193-209, DOI: 10.1016/S0012-821X(02)00472-7, 2002.

Martinot, C., Bolton, C.T., Sarr, A.C., Donnadieu, Y., Garcia, M., Gray, E. and Tachikawa, K.: Drivers of late Miocene tropical sea surface cooling: A new perspective from the equatorial Indian Ocean. Paleoceanography and Paleoclimatology, 37(10), p.e2021PA004407, 2022.

Mashiotta, T. A., Lea, D. W., and Spero, H. J.: Glacial–interglacial changes in Subantarctic sea surface temperature and δ18O-water using foraminiferal Mg, Earth and Planetary Science Letters, 170, 417-432, https://doi.org/10.1016/S0012-821X(99)00116-8, 1999.

Mawbey, E. M. and Lear, C. H.: Carbon cycle feedbacks during the Oligocene-Miocene transient glaciation, Geology, 41, 963-966, 10.1130/g34422.1, 2013.

Meckler, A. N., Sexton, P. F., Piasecki, A. M., Leutert, T. J., Marquardt, J., Ziegler, M., Agterhuis, T., Lourens, L. J., Rae, J. W. B., Barnet, J., Tripati, A., and Bernasconi, S. M.: Cenozoic evolution of deep ocean temperature from clumped isotope thermometry, Science, 377, 86-90, 10.1126/science.abk0604, 2022.

Mucci, A. and Morse, J. W.: The incorporation of Mg2+ and Sr2+ into calcite overgrowths: influences of growth rate and solution composition, Geochimica et Cosmochimica Acta, 47, 217-233, https://doi.org/10.1016/0016-7037(83)90135-7, 1983.

Nairn, M.G., Lear, C.H., Sosdian, S.M., Bailey, T.R., Beavington-Penney, S.: Tropical sea surface temperatures following the middle Miocene climate transition from laser-ablation ICP-MS analysis of glassy foraminifera. Paleoceanography and Paleoclimatology, 36, e2020PA004165. doi:10.1029/2020PA004165, 2021.

Nathan, S. A., and Leckie, R. M.: Early history of the Western Pacific Warm Pool during the middle to late Miocene (~13.2-5.8 Ma): Role of sea-level change and implications for equatorial circulation. Palaeogeography, Palaeoclimatology, Palaeoecology, 274(3-4), 140-159, doi:10.1016/j.palaeo.2009.01.007, 2009.

https://doi.org/10.5194/essd-2026-697
Preprint. Discussion started: 18 September 2026

Nauter-Alves, A., Evans, D., Katz, M. E., Gray, W. R., Rae, J. W. B., and Borrelli, C.: Thermal and Non-Thermal Controls on Benthic Foraminiferal Mg/Ca, Sr/Ca, B/Ca, and Mg/Li: Global Core-Top Compilation, Revised Calibrations, and Application to the Geologic Record, Paleoceanography and Paleoclimatology, 40, e2025PA005176, https://doi.org/10.1029/2025PA005176, 2025.

Nürnberg, D., Bijma, J., and Hemleben, C.: Assessing the reliability of magnesium in foraminiferal calcite as a proxy for water mass temperatures. Geochimica et Cosmochimica Acta, 60(5), 803–814. https://doi.org/10.1016/0016-7037(95)00446-7, 1996.

Pälike, H., Lyle, M. W., Nishi, H., Raffi, I., Ridgwell, A., Gamage, K., Klaus, A., Acton, G., Anderson, L., Backman, J., Baldauf, J., Beltran, C., Bohaty, S. M., Bown, P., Busch, W., Channell, J. E. T., Chun, C. O. J., Delaney, M., Dewangan, P., Dunkley Jones, T., Edgar, K. M., Evans, H., Fitch, P., Foster, G. L., Gussone, N., Hasegawa, H., Hathorne, E. C., Hayashi, H., Herrle, J. O., Holbourn, A., Hovan, S., Hyeong, K., Iijima, K., Ito, T., Kamikuri, S.-i., Kimoto, K., Kuroda, J., Leon-Rodriguez, L., Malinverno, A., Moore Jr, T. C., Murphy, B. H., Murphy, D. P., Nakamura, H., Ogane, K., Ohneiser, C., Richter, C., Robinson, R., Rohling, E. J., Romero, O., Sawada, K., Scher, H., Schneider, L., Sluijs, A., Takata, H., Tian, J., Tsujimoto, A., Wade, B. S., Westerhold, T., Wilkens, R., Williams, T., Wilson, P. A., Yamamoto, Y., Yamamoto, S., Yamazaki, T., and Zeebe, R. E.: A Cenozoic record of the equatorial Pacific carbonate compensation depth, Nature, 488, 609-614, 10.1038/nature11360, 2012.

Pearson, P. N. and Burgess, C. E.: Foraminifer test preservation and diagenesis: comparison of high latitude Eocene sites, Geological Society, London, Special Publications, 303, 59-72, doi:10.1144/SP303.5, 2008.

Pearson, P. N., and Wade, B. S.: Taxonomy and stable isotope paleoecology of well-preserved planktonic foraminifera from the uppermost Oligocene of Trinidad, *J. Foram. Res.*, **39**, 191–217, https://doi.org/10.2113/gsjfr.39.3.191, 2009.

Pearson, P. N. and Shackleton, N. J.: Neogene Multispecies planktonic foraminifer stable isotope record, Site 871, Limalok Guyot, Proceedings of the Ocean Drilling Program, Scientific Results, 144, 401 - 407, 1995.

Pearson, P. N., Ditchfield, P.W., Singano, J., Harcourt-Brown, K., Nicholas, C.J., Olsson, R.K., Shackleton, N.J., Hall, M.A.: Warm tropical sea surface temperatures in the Late Cretaceous and Eocene epochs, Nature, 413 (6855), 481-487, doi: 10.1038/35097000, 2001.

Pena, L. D., Calvo, E., Cacho, I., Eggins, S., and Pelejero, C.: Identification and removal of Mn-Mg-rich contaminant phases on foraminiferal tests: Implications for Mg/Ca past temperature reconstructions, Geochemistry, Geophysics, Geosystems, 6, https://doi.org/10.1029/2005GC000930, 2005.

Raitzsch, M., Bijma, J., Bickert, T., Schulz, M., Holbourn, A., and Kučera, M.: Atmospheric carbon dioxide variations across the middle Miocene climate transition, Clim. Past, 17, 703–719, https://doi.org/10.5194/cp-17-703-2021, 2021.

Raitzsch, M., Kuhnert, H., Groeneveld, J., and Bickert, T.: Benthic foraminifer Mg/Ca anomalies in South Atlantic core top sediments and their implications for paleothermometry. Geochemistry, Geophysics, Geosystems, 9(5), Q05010, https://doi.org/10.1029/2007GC001788, 2008.

Rausch, S., Böhm, F., Bach, W., Klügel, A., and Eisenhauer, A.: Calcium carbonate veins in ocean crust record a threefold increase of seawater Mg/Ca in the past 30 million years, Earth and Planetary Science Letters 362, 215-224, https://doi.org/10.1016/j.epsl.2012.12.005, 2013.

Regenberg, M., Regenberg, A., Garbe-Schönberg, D., and Lea, D.W.: Global dissolution effects on planktonic foraminiferal Mg/Ca ratios controlled by the calcite-saturation state of bottom waters, Paleoceanography, 29, 127–142, doi:10.1002/2013PA002492, 2014.

Ries, J. B.: Effect of ambient Mg/Ca ratio on Mg fractionation in calcareous marine invertebrates: A record of the oceanic Mg/Ca ratio over the Phanerozoic, Geology, 32, 981-984, 10.1130/G20851.1, 2004.

Rongstad, B. L., Marchitto, T. M., and Herguera, J. C.: Understanding the Effects of Dissolution on the Mg/Ca Paleothermometer in Planktic Foraminifera: Evidence From a Novel Individual Foraminifera Method, Paleoceanography, 32, 1386-1402, https://doi.org/10.1002/2017PA003179, 2017.

Rosenthal, Y., Perron-Cashman, S., Lear, C. H., Bard, E., Barker, S., Billups, K., Bryan, M., Delaney, M. L., deMenocal, P. B., Dwyer, G. S., Elderfield, H., German, C. R., Greaves, M., Lea, D. W., Marchitto Jr, T. M., Pak, D. K., Paradis, G. L., Russell, A. D., Schneider, R. R., Scheiderich, K., Stott, L., Tachikawa, K., Tappa, E., Thunell, R., Wara, M., Weldeab, S., and Wilson, P. A.: Interlaboratory comparison study of Mg/Ca and Sr/Ca measurements in planktonic foraminifera for paleoceanographic research, Geochemistry, Geophysics, Geosystems, 5, https://doi.org/10.1029/2003GC000650, 2004.

Rosenthal, Y., Holbourn, A.E., Kulhanek, D.K., and the Expedition 363 Scientists: Western Pacific Warm Pool. Proceedings of the International Ocean Discovery Program, 363, College Station, TX (International Ocean Discovery Program). doi 10.14379/iodp.proc.363.201, 2018.

Rosenthal, Y., Lear, C. H., D. W. Oppo, D. W., and Linsley, B. K.: Temperature and carbonate ion effects on Mg/Ca and Sr/Ca ratios in benthic foraminifera: Aragonitic species Hoeglundina elegans, Paleoceanography, 21, PA1007, DOI:10.1029/2005PA001158, 2006.

Rosenthal, Y., Bova, S., and Zhou, X.: A user guide for choosing planktic foraminiferal Mg/Ca-temperature calibrations. Paleoceanography and Paleoclimatology, 37, e2022PA004413, https://doi.org/10.1029/2022PA004413, 2022.

Sato, T., Oda, M., Chiyonobu, S., Kimoto, K., Domitsu, H., and Ingle Jr., J. C.: Establishment of the western Pacific warm pool during the Pliocene: Evidence from planktic foraminifera, oxygen isotopes, and Mg/Ca ratios. Palaeogeography, Palaeoclimatology, Palaeoecology, 265(1-2), 140-147, https://doi.org/10.1016/j.palaeo.2008.05.003, 2008.

Scheiner, F., Holcová, K., Milovský, R., and Kuhnert, H.: Temperature and isotopic composition of seawater in the epicontinental sea (Central Paratethys) during the Middle Miocene Climate Transition based on Mg/Ca, $\delta^{18}O$ and $\delta^{13}C$ from foraminiferal tests. Palaeogeography, Palaeoclimatology, Palaeoecology, 495, 60-71, https://doi.org/10.1016/j.palaeo.2017.12.027, 2018

Segev, E., and Erez, J.: Effect of Mg/Ca ratio in seawater on shell composition in shallow benthic foraminifera, Geochem. Geophys. Geosyst., 7, Q02P09, DOI:10.1029/2005GC000969, 2006

Sexton, P. F. and Wilson, P. A.: Preservation of benthic foraminifera and reliability of deep-sea temperature records: Importance of sedimentation rates, lithology, and the need to examine test wall structure, Paleoceanography, 24, https://doi.org/10.1029/2008PA001650, 2009.

Sexton, P. F., Wilson, P. A., and Pearson, P. N.: Microstructural and geochemical perspectives on planktic foraminiferal preservation: “Glassy” versus “Frosty”, Geochemistry, Geophysics, Geosystems, 7, https://doi.org/10.1029/2006GC001291, 2006.

Shevenell, A. E., Kennett, J. P., and Lea, D. W.: Middle Miocene Southern Ocean cooling and Antarctic cryosphere expansion. Science, 305(5691), 1766-1770, DOI:10.1126/science.1100061, 2004.

Shevenell, A. E., Kennett, J. P., and Lea, D. W.: Middle Miocene ice sheet dynamics, deep-sea temperatures, and carbon cycling: A Southern Ocean perspective. Geochemistry, Geophysics, Geosystems, 9, Q02006. doi:10.1029/2007GC001736, 2008.

https://doi.org/10.5194/essd-2026-697
Preprint. Discussion started: 18 September 2026

Open Access Earth System Science Data Discussions

Spezzaferri, S., Kucera, M., Pearson, P. N., Wade, B. S., Rapp, S., Poole, C. R., et al: Fossil and genetic evidence for the polyphyletic nature of the planktonic foraminifera "*Globigerinoides*", and description of the new genus *Trilobatus*, *PLoS ONE*, **10**, e0128108, https://doi.org/10.1371/journal.pone.0128108, 2015.

Spezzaferri, S., Coxall, H. K., Olsson, R. K., and Hemleben, C.: Taxonomy, biostratigraphy, and phylogeny of Oligocene *Globigerina*, *Globigerinella*, and *Quiltyella* n. gen., in: *Atlas of Oligocene Planktonic Foraminifera*, Cushman Foundation for Foraminiferal Research, 2018a.

Spezzaferri, S., Olsson, R. K., Hemleben, C., Wade, B. S., and Coxall, H. K.: Taxonomy, biostratigraphy, and phylogeny of Oligocene and lower Miocene *Globoturborotalita*, in: *Atlas of Oligocene Planktonic Foraminifera*, Cushman Foundation for Foraminiferal Research, 2018b.

Sosdian, S., Auderset, A., Modestou, S., Holbourn, A., and the MioOcean Working Group: *MioOcean temperature compilation,* Zenodo [data set],https://doi.org/10.5281/zenodo.22258386, 2026.

Sosdian et al., this volume refers to ESSD companion paper with the following manuscript information: Sindia M. Sosdian, Alexandra Auderset, Sevasti Modestou, Ann Holbourn, Flavia Boscolo-Galazzo, Anna Joy Drury, Anya V. Hess, Karlos G. D. Kochhann, Diederik Liebrand, Xiaoqing Liu, Jared Nirenberg, Neeraj S. Shah, Deborah N. Tangunan, Gerald Auer, Marcus P. S. Badger, Clara Bolton, Alexander Clark, Anya J. Crocker, David Evans, Sarah Feakins, Timothy Herbert, Emily Judd, Jennifer Kasbohm, David J. King, Wout Krijgsman, Wolfgang Kuhnt, Kira Lawrence, Caroline H. Lear, Kim Marshall-Mills, Erin McClymont, Nele Meckler, Paul Minton, Katrina Nilsson-Kerr, Diana Ochoa, Marci M. Robinson, Thamizharasan Sakthivel, Francesca Sangiorgi, Amelia E. Shevenell, Weimin Si, Elizabeth C. Sibert, Kasia K. Sliwinska, Appy Sluijs, Heather Stoll, Victoria Taylor, Tim van Peer, Bridget S. Wade, Thomas Westerhold, Evi Wubben, Yige Zhang, and Martin Ziegler: MioOcean: database compilation and temperature proxy systematics in the Miocene oceans. ESSD Manuscript Reference essd-2026-699.

Sosdian, S. M., Greenop, R., Hain, M. P., Foster, G. L., Pearson, P. N., and Lear, C. H.: Constraining the evolution of Neogene ocean carbonate chemistry using the boron isotope pH proxy. Earth and Planetary Science Letters, 498, 362-376. doi:10.1016/j.epsl.2018.06.017, 2018.

Sosdian, S. M., Babila, T. L., Greenop, R., Foster, G. L., and Lear, C.H.: Ocean Carbon Storage across the middle Miocene: a new interpretation for the Monterey Event, Nature Communications 11, Article number 134, https://doi.org/10.1038/s41467-019-13792-0, 2020.

Sosdian, S. M. and Lear, C. H.: Initiation of the Western Pacific Warm Pool at the Middle Miocene Climate Transition?, Paleoceanography and Paleoclimatology, 35, e2020PA003920, https://doi.org/10.1029/2020PA003920, 2020.

Sosdian, S., Coxall, H., Steinthorsdottir, M., and Lawrence, K.: Miocene temperature portal. Dataset version 4. Bolin Centre Database. https://doi.org/10.17043/miocene-temperature-portal-4, 2024.

Steinthorsdottir, M., Coxall, H. K., de Boer, A. M., Huber, M., Barbolini, N., Bradshaw, C. D., Burls, N. J., Feakins, S. J., Gasson, E., Henderiks, J., Holbourn, A. E., Kiel, S., Kohn, M. J., Knorr, G., Kürschner, W. M., Lear, C. H., Liebrand, D., Lunt, D. J., Mörs, T., Pearson, P. N., Pound, M. J., Stoll, H., and Strömberg, C. A. E.: The Miocene: The future of the past, Paleoceanography and Paleoclimatology, 36, e2020PA004037. https://doi.org/10.1029/2020PA004037, 2021.

Steinke, S., Groeneveld, J., Johnstone, H., and Rendle-Bühring, R.: East Asian summer monsoon weakening after 7.5 Ma: Evidence from combined planktonic foraminifera Mg/Ca and d^{18}O (ODP Site 1146, northern South China Sea). Palaeogeography, Palaeoclimatology, Palaeoecology, 289(1-4), 33-43, DOI:10.1016/j.palaeo.2010.02.007, 2010.

Staudigel, P. T., John, E. H., Buse, B., Pearson, P. N., and Lear, C. H.: Apparent preservation of primary foraminiferal Mg/Ca ratios and Mg-banding in recrystallized foraminifera, Geology, 50, 760-764, 10.1130/g49984.1, 2022.

https://doi.org/10.5194/essd-2026-697
Preprint. Discussion started: 18 September 2026

Thomas, E.: Late Cretaceous through Neogene deep-sea benthic foraminifers, Maud Rise, Weddell Sea, Antarctica, Proc. Ocean Drill. Program Sci. Results, 113, 571–594, 1990.

Tierney, J.E., Malevich, S.B., Gray, W., Vetter, L., and Thirumalai, K.: Bayesian calibration of the Mg/Ca paleothermometer in planktic foraminifera, Paleoceanography and Paleoclimatology, 34, 2005-2030, https://doi.org/10.1029/2019PA003744, 2019.

Tjalsma, R.C., and Lohmann, G.P., 1983. *Paleocene–Eocene Bathyal and Abyssal Benthic Foraminifera from the Atlantic Ocean.* Micropaleontology, Spec. Publ., 4:1–90

Verducci, M., Foresi, L., Scott, G., Tiepolo, Sprovieri, M., and Lirer, F., 2007, East Antarctic Ice Sheet fluctuations during the Middle Miocene Climatic Transition inferred from faunal and biogeochemical data on planktonic foraminifera (ODP Hole 747A, Kerguelen Plateau): U.S. Geological Survey Open-File Report 2007-1047-SRP-037, 5 pp., https://doi.org/10.3133/ofr20071047SRP037, 2007

Verducci, M., Foresi, L. M., Scott, G. H., Sprovieri, M., Lirer, F., Pelosi, N.: The Middle Miocene climatic transition in the Southern Ocean: Evidence of paleoclimatic and hydrographic changes at Kerguelen plateau from planktonic foraminifers and stable isotopes, Palaeogeography, Palaeoclimatology, Palaeoecology, 280, 371–386, DOI:10.1016/j.palaeo.2009.06.024, 2009.

Wade, B. S., Pearson, P. N., Berggren, W. A., and Pälike, H.: Review and revision of Cenozoic tropical planktonic foraminiferal biostratigraphy and calibration to the geomagnetic polarity and astronomical time scale, Earth-Science Reviews, 104, 111-142, https://doi.org/10.1016/j.earscirev.2010.09.003, 2011.

Whiteford, R., Heaton, T. J., Henehan, M. J., Anagnostou, E., Jurikova, H., Foster, G. L., and Rae, J. W. B.: Reconstruction of Cenozoic δ11Bsw Using a Gaussian Process, Paleoceanography and Paleoclimatology, 39, e2023PA004769, https://doi.org/10.1029/2023PA004769, 2024.

Wilson, P., and Norris, R. Warm tropical ocean surface and global anoxia during the mid-Cretaceous period, Nature, 412, 425–429, https://doi.org/10.1038/35086553, 2001.

Yang, C., Dang, H., Zhou, X., Zhang, H., Wang, X., Wang, Y., Qiao, P., Jiang, X., and Jian, Z.: Upper ocean hydrographic changes in response to the evolution of the East Asian monsoon in the northern South China Sea during the middle to late Miocene. Global and Planetary Change, 103478. DOI:10.1016/j.gloplacha.2021.103478, 2021.

Yang, C., Dang, H., Zhang, P., Xu, J., and Jian, Z.: Surface-ocean hydrographic variability in the northern South China Sea across the Miocene Climatic Optimum, Palaeogeography, Palaeoclimatology, Palaeoecology, 697, 113901, https://doi.org/10.1016/j.palaeo.2026.113901, 2026.

Yang, X., Groeneveld, J., Jian, Z., Steinke, S., and Giosan, L.: Middle Miocene intensification of South Asian monsoonal rainfall. Paleoceanography and Paleoclimatology, 35, e2020PA003853. https://doi.org/10.1029/2020PA003853, 2020.

Yu, J., Elderfield, H., Greaves, M., and Day, J.: Preferential dissolution of benthic foraminiferal calcite during laboratory reductive cleaning, Geochemistry, Geophysics, Geosystems, 8, https://doi.org/10.1029/2006GC001571, 2007.

Yu, J., and Elderfield, H.: Mg/Ca in the benthic foraminifera *Cibicidoides wuellerstorfi* and *Cibicidoides mundulus*: Temperature versus carbonate ion saturation. Earth and Planetary Science Letters, 276, 129–139, DOI:10.1016/j.epsl.2008.09.015, 2008.

Zhou, X., Rosenthal, Y., Haynes, L., Si, W., Evans, D., Huang, K.-F., and Erez, J.: Planktic foraminiferal Na/Ca: A potential proxy for seawater calcium concentration. Geochimica et Cosmochimica Acta, 305, 306–322. https://doi.org/10.1016/j.gca.2021.04.012, 2021.

Zou, S., Groeneveld, J., Giosan, L., and Steinke S.: Determining the habitat depth of the planktic foraminifera Dentoglobigerina altispira in the eastern Arabian Sea during the middle Miocene. Marine Micropaleontology, 170, 102075. DOI:10.1016/j.marmicro.2021.102075, 2022.